

1  
2  
3  
4  
5  
6  
7  
8  
9  
10  
11  
12  
13  
14  
15  
16  
17  
18  
19  
20  
21  
22  
23  
24  
25  
26  
27  
28  
29  
30  
31

**Title: Translational gene expression control in *Chlamydia trachomatis*.**

Nicole A Grieshaber<sup>1</sup>, Travis J Chiarelli, Cody R Appa<sup>1</sup>, Grace Neiswanger<sup>1</sup>, Kristina Peretti<sup>1</sup>, Scott S Grieshaber<sup>1\*</sup>

<sup>1</sup>Department of Biological Sciences, University of Idaho, Moscow, ID, USA.

\*Corresponding Author:  
Scott Grieshaber, Ph.D.  
Associate Professor  
Department of Biological Sciences  
University of Idaho  
875 Perimeter Drive MS 3051  
Moscow, ID 83844

32

33

34 **Abstract:**

35 The human pathogen *Chlamydia trachomatis* proceeds through a multi phenotypic  
36 developmental cycle with each cell form specialized for different roles in pathogenesis.  
37 Understanding the mechanisms regulating this complex cycle has historically been  
38 hampered by limited genetic tools. In an effort to address this issue, we developed a  
39 translational control system to regulate gene expression in *Chlamydia* using a synthetic  
40 riboswitch. Here we demonstrate that translational control via a riboswitch can be used in  
41 combination with a wide range of promoters in *C. trachomatis*. The synthetic riboswitch  
42 E, inducible with theophylline, was used to replace the ribosome binding site of the  
43 synthetic promoter T5-lac, the native chlamydial promoter of the *pgp4* plasmid gene and  
44 an anhydrotetracycline responsive promoter. In all cases the riboswitch inhibited  
45 translation, and high levels of protein expression was induced with theophylline.  
46 Combining the Tet transcriptional inducible promoter with the translational control of the  
47 riboswitch resulted in strong repression and allowed for the cloning and expression of the  
48 potent chlamydial regulatory protein, HctB. The ability to control the timing and strength  
49 of gene expression independently from promoter specificity is a new and important tool  
50 for studying chlamydial regulatory and virulence genes.

51

## 52 **Introduction:**

53 The bacterial species *Chlamydia trachomatis* (*Ctr*), are a group of human pathogens  
54 composed of over 15 distinct serovars causing trachoma, the leading cause of  
55 preventable blindness, and sexually acquired infections of the urogenital tract. According  
56 to the CDC, *Ctr* is the most frequently reported sexually transmitted infection in the United  
57 States, costing the American healthcare system nearly \$2.4 billion annually [1,2]. These  
58 infections are widespread among all age groups and ethnic demographics, infecting ~3%  
59 of the human population worldwide [3]. In women, untreated genital infections can result  
60 in devastating consequences such as pelvic inflammatory disease, ectopic pregnancy,  
61 and infertility [4,5]. Every year, there are over 4 million new cases of *Chlamydia* in the  
62 United States [6,7] and an estimated 152 million cases worldwide [8]. Understanding the  
63 genetic factors that mediate infection and disease has historically been hindered by the  
64 lack of good genetic tools. This has changed dramatically in the last few years with  
65 advances in chlamydial transformation. The ability to introduce genetically manipulatable  
66 plasmids into *Ctr* has created multiple opportunities to bring genetic manipulation  
67 techniques to the field [9–11]. The ability to alter the expression levels and timing of  
68 proteins involved in chlamydial pathogenesis is an important tool in teasing apart the  
69 mechanisms that control chlamydial infections.

70 Here we demonstrate the use of an inducible translational control system using a  
71 synthetic riboswitch in *Ctr*. Riboswitches are naturally occurring mRNA elements that  
72 regulate gene expression in all domains of life [12]. In bacteria, riboswitches generally  
73 function to interfere with translation of the mRNA. Riboswitches contain an aptamer  
74 sequence that binds a cognate ligand causing the mRNA to adopt an alternative  
75 secondary-structure conformation. In bacteria, the changes in mRNA secondary structure  
76 can control the availability of the ribosome binding site on the mRNA. A collection of  
77 synthetic riboswitches was recently developed through screening and rational design [13].  
78 These riboswitches respond to theophylline, a caffeine analog, and function through a  
79 translation initiation mechanism. We successfully adapted one of these theophylline  
80 inducible riboswitches, termed E riboswitch, to control gene expression in *Ctr*.  
81 Additionally, we demonstrated that translational control can be used in conjunction with  
82 constitutive promoters, inducible promoters and native chlamydial promoters,  
83 demonstrating the versatility of translational inducible control of gene expression in a  
84 variety of use cases.

85

## 86 **Material and Methods:**

87

### 88 **Cell Culture**

89 Cell lines were obtained from the American Type Culture Collection. Cos-7 cells (CRL-  
90 1651) were grown in RPMI-1640, supplemented with 10% FBS and 10 µg/mL gentamicin  
91 (Cellgro). *Chlamydia trachomatis* serovar L2 (LGV Bu434) was grown in Cos-7 cells.

92 Elementary Bodies (EBs) were purified by density gradient (DG) centrifugation essentially  
93 as described [37] following 43-45 h of infection. EBs were stored at -80°C in Sucrose  
94 Phosphate Glutamate (SPG) buffer (10 mM sodium phosphate [8mM K<sub>2</sub>HPO<sub>4</sub>, 2mM  
95 KH<sub>2</sub>PO<sub>4</sub>], 220 mM sucrose, 0.50 mM l-glutamic acid, pH 7.4) until use.

96

## 97 **Vector Construction**

98 All *Ctr* expression constructs used p2TK2-SW2 [20]. as the backbone and all cloning was  
99 performed using the In-fusion HD EcoDry Cloning kit (FisherScientific). All primers and  
100 geneblocks (gBlocks) were ordered from Integrated DNA Technologies (IDT) and are  
101 noted in Table ST1.

### 102 p2TK2-SW2-T5-E-clover-3xflag

103 An E-clover-3xFlag fragment was ordered as a gBlock and inserted between the T5  
104 promoter and IncD terminator of p2TK2-SW2 to generate p2TK2-SW2-E-clover-3xFlag.  
105 The backbone was generated using primers 5' E-clover-Flag bb and 3' E-clover-Flag bb.

### 106 p2TK2-SW2-E-hctB-3xFlag

107 The *hctB* ORF was amplified from *Ctr* L2(434) using the primers indicated in Table ST1.  
108 The fragment was used to replace Clover in p2TK2-SW2- E-clover-3xFlag. The primers  
109 used to generate the backbone are described in Table ST1.

### 110 p2TK2-SW2-Tet-J-E-clover-3xflag

111 A gBlock encoding the Tet repressor, Tet promoter and the riboJ ribozyme insulator  
112 (Table ST1) was inserted upstream of the E riboswitch of p2TK2-SW2-E-clover-3xFlag,  
113 replacing the T5 promoter.

### 114 p2TK2-SW2-Tet-J-E-hctB-3xFlag

115 The *hctB* ORF was amplified from *Ctr* L2(434) using the primers 5' Tet-J-HctBi and 3' Tet-  
116 J-HctBi. The fragment was used to replace Clover in p2TK2-SW2 -Tet-J-E-clover-3xFlag.

### 117 p2TK2-SW2-*nprom*-E-pgp4-3xFlag

118 An E-pgp4-3xFlag fragment was ordered as a gBlock and inserted between the *pgp4*  
119 native promoter and the IncD terminator of p2TK2-SW2. The backbone was generated  
120 using the primers indicated in Table ST1.

### 121 p2TK2-SW2-T5-E-ngLVA-3xFlag and p2TK2-SW2-Tet-J-E-ngLVA-3xFlag

122 A neongreenLVA (ngLVA) fragment was ordered as a gBlock from IDT and inserted to  
123 replace Clover of both p2TK2-SW2-E-clover-3xFlag and p2TK2-SW2-Tet-J-E-clover-  
124 3xflag. The primers indicated in Table ST1 were used for both plasmids to generate the  
125 back bone.

### 126 p2TK2-SW2-euoprom-ngLVA

127 The primers 5' ngLVAi and 3' ngLVAi (Table ST1) were used to amplify the ngLVA  
128 fragment from E-ngLVA-3xFlag and inserted to replace Clover of euoprom-Clover [23].  
129 The primers indicated in Table ST1 were used to generate the back bone.

130

## 131 **Chlamydial Transformation and Isolation.**

132 Transformation of Ctr L2 was performed essentially as previously described [38]. Briefly,  
133  $1 \times 10^8$  EBs +  $>2 \mu\text{g}$  DNA/well were used to infect a 6 well plate. Transformants were  
134 selected over successive passages with 1U/ml Penicillin G or 500 $\mu\text{g}/\text{ml}$  Spectinomycin  
135 as appropriate for each plasmid. The new strain was clonally isolated via successive  
136 rounds of inclusion isolation (MOI,  $<1$ ) using a micromanipulator. Clonality of each strain  
137 was confirmed by isolating the plasmid, transforming into *E. coli* and sequencing six  
138 transformants.

139

## 140 **Fluorescence Staining**

141 *Cos7* cells on coverslips were infected with the indicated strains. Protein expression  
142 regulated by the E-riboswitch only were induced at 16 hpi with 0.5mM theophylline (Acros  
143 Organics, Thermo Scientific™). Protein expression regulated by both the Tet promoter  
144 and the E-riboswitch were induced at 16 hpi with 0.5mM theophylline and 30ng/ml  
145 anhydroTetracycline (Acros Organics, Thermo Scientific™). Samples were fixed with 4%  
146 buffered paraformaldehyde at 24 hpi and stained with Monoclonal anti-Flag M2 antibody  
147 (1:500, Sigma, Thermo Scientific™) and alexa 488 anti-mouse secondary antibody to  
148 visualize expressing Chlamydia. DAPI was used to visualize DNA. Coverslips were  
149 mounted on a microscope slide with a MOWIOL® mounting solution (100 mg/mL  
150 MOWIOL® 4-88, 25% glycerol, 0.1 M Tris pH 8.5).

151 Fluorescence images were acquired using a Nikon spinning disk confocal system  
152 with a 60x oil-immersion objective, equipped with an Andor Ixon EMCCD camera, under  
153 the control of the Nikon elements software. Images were processed using the image  
154 analysis software ImageJ (<http://rsb.info.nih.gov/ij/>). Representative confocal  
155 micrographs displayed in the figures are maximal intensity projections of the 3D data sets,  
156 unless otherwise noted.

157

## 158 **Live cell imaging**

159 Infected monolayers of *Cos7* cells grown in a glass bottom 24 well plate were induced at  
160 16 hpi with either 0.5mM theophylline only or the indicated concentrations of theophylline  
161 and anhydroTetracycline. Plates were imaged immediately upon induction.

162 Live cell imaging was achieved using an automated Nikon epifluorescent microscope  
163 equipped with an Okolab (<http://www.oko-lab.com/live-cell-imaging>) temperature  
164 controlled stage and an Andor Zyla sCMOS camera (<http://www.andor.com>). Images  
165 were taken every fifteen minutes for a further 36 hours. Multiple fields of view of multiple  
166 wells were imaged. The fluorescence intensity of each inclusion over time was tracked  
167 using the ImageJ plugin Trakmate [39]. and the results were averaged and plotted using  
168 python and matplotlib [23]

169

## 170 **Replating Assay.**

171 *Chlamydia* were isolated by scraping the infected monolayer into media and pelleting at  
172 17200 rcfs. The EB pellets were resuspended in RPMI via sonication and seeded onto  
173 fresh monolayers in a 96-well microplate in a 2-fold dilution series. Infected plates were  
174 incubated for 24 hours prior to fixation with methanol and stained with DAPI and  
175 *Chlamydia trachomatis* MOMP Polyclonal Antibody, FITC (Fishersci). The DAPI stain  
176 was used for automated microscope focus and visualization of host-cell nuclei and the  
177 anti-*Ctr* antibody for visualization of EBs and inclusion counts. Inclusions were imaged  
178 using a Nikon Eclipse TE300 inverted microscope utilizing a scopeLED lamp at 470nm  
179 and 390nm, and BrightLine band pass emissions filters at 514/30nm and 434/17nm.  
180 Image acquisition was performed using an Andor Zyla sCMOS in conjunction with  
181  $\mu$ Manager software. Images were analyzed using ImageJ software and custom scripts.  
182 Statistical comparisons between treatments were performed using an ANOVA test  
183 followed by Tukey's Honest Significant Difference test.

184

### 185 **Western Analysis**

186 Infected monolayers were lysed in reducing lane marker sample buffer and protein lysates  
187 were separated on 12% SDS-PAGE gels and transferred to a Nitrocellulose Membrane  
188 for western analysis. The membrane was blocked with PBS + 0.1% Tween 20 (PBS-T)  
189 and 5% nonfat milk prior to incubating in monoclonal anti-Flag M2 antibody (1:10,000,  
190 Sigma, Thermo Scientific™) overnight at 4 °C followed by Goat-anti Mouse IgG-HRP  
191 secondary antibody (Invitrogen™) at room temperature for 2 hours. The membrane was  
192 developed with the Supersignal West Dura luminol and peroxide solution (Thermo  
193 Scientific™) and imaged using an Amersham Imager 600.

194

### 195 **Glycogen staining**

196 Monolayers were infected with the indicated strains and induced with 0.5mM theophylline  
197 at the time of infection. At 40 hpi, the media was removed and the samples were stained  
198 with 1 ml of a 1:50 dilution of 5% iodine stain (5% potassium iodide and 5% iodine in  
199 50% ethanol) in PBS for 10 min. Samples were then stained in 1:50 Lugol's iodine solution  
200 in PBS (10% potassium iodide and 5% iodine in ddH<sub>2</sub>O) and imaged directly. Images  
201 were acquired using a Nikon microscope using phase brightfield illumination and an  
202 Andor Zyla sCMOS camera.

203

### 204 **RNA-Seq**

205 Total RNA was isolated from cells infected with L2-Tet-J-E-hctB-flag. Expression of HctB  
206 was induced with 0.5 mM theophylline and 30ng/ml aTc at 15 hpi and the *Chlamydia*  
207 isolated at 24 hpi on ice. Briefly, the infected monolayer was scraped into ice cold PBS,  
208 lysed using a Dounce homogenizer and the *Chlamydia* isolated over a 30% MD-76R pad.  
209 Total RNA was isolated using TRIzol reagent (Life Technologies) following the protocol



210 provided and genomic DNA removed (TURBO DNA-free Kit, Invitrogen). The enriched  
211 RNA samples were quantified and the libraries built and barcoded by the IBEST  
212 Genomics Resources Core at the University of Idaho. The libraries were sequenced by  
213 University of Oregon sequencing core using the Illumina NovaSeq platform. RNA-seq  
214 reads were aligned to the published *C. trachomatis* L2 Bu 434 genome using the bowtie2  
215 aligner software [40]. Reads were quantified using HTseq [41] Statistical analysis and  
216 normalization of read counts was accomplished using DESeq2 in R [42]. Log2fold  
217 change and statistics were also calculated using DESeq2. Heatmaps and hierarchical  
218 clustering were generated and visualized using python with pandas and the seaborn  
219 visualization package [43]. Aligned reads are accessible from the NCBI's Sequence Read  
220 Archive (SRA) submission number SUB10220676.

221

## 222 **Results:**

223

### 224 **Translational control of gene expression from a synthetic constitutive** 225 **promoter.**

226 Controlling the timing and level of gene expression is an important tool for uncovering the  
227 function of genes that are involved in chlamydial pathogenesis. We developed an  
228 inducible expression system for use in *C. trachomatis* using a synthetic riboswitch that  
229 binds the small molecule theophylline [14,15]. We used the synthetic riboswitch E behind  
230 a T5-lac promoter (T5) to drive expression of the GFP variant, Clover [16,17] (Fig. 1A).  
231 The T5-lac promoter is a hybrid promoter made from the phage T5 early promoter and  
232 the lac-operon [18]. The E riboswitch when not bound to theophylline folds to block the  
233 initiation of translation [19]. However, when the riboswitch binds theophylline the  
234 ribosome binding site is no longer obscured by the RNA secondary structure allowing for  
235 efficient translation. A T5-E-clover-3xFlag fragment was cloned into the chlamydial  
236 plasmid p2TK2-SW2 [20,21] to make the p2TK2-SW2-T5-E-clover-3xflag plasmid (Fig.  
237 1A) and transformed into *Ctr* L2 454 resulting in the strain L2-E-clover-flag. Cos-7 cells  
238 were infected with these transformants and Clover expression was evaluated by western  
239 blotting. Cells were infected and treated with either theophylline or vehicle at 16 hours  
240 post infection (hpi) and cell lysates were analyzed for protein production at 30 hpi. Clover  
241 expression was quite tightly regulated and was only detectable in the theophylline treated  
242 sample (Fig. 1B). In addition to western blotting we also evaluated the expression of  
243 Clover using confocal microscopy. Cos-7 cells grown on coverslips were infected with the  
244 L2-E-clover-flag strain and Clover expression was induced with theophylline at 16 hpi.  
245 The coverslips were fixed at 30 hpi and imaged for Clover expression using confocal  
246 microscopy. Again, only inclusions treated with theophylline had fluorescent *Chlamydia*  
247 (Fig. 1C).

248

249 **Figure 1. Characterization of p2TK2-SW2-T5-E-clover-flag.** A) Schematic of the E-  
250 clover expression construct consisting of the T5-lac promoter (T5), riboE riboswitch (rsE)  
251 and the ORF for the clover fluorescent protein with an inframe 3x flag tag. B) Anti-flag  
252 western blot of Cos-7 cells infected with L2-T5-E-clover-flag comparing expression of  
253 theophylline treated and untreated cultures. Cells were induced or not with 0.5 mM  
254 theophylline at 16 hpi and proteins were harvested at 30 hpi. C) Confocal micrographs of  
255 Cos-7 cells infected with L2-T5-E-clover-flag and induced or not with 0.5 mM theophylline  
256 at 16 hpi and fixed and stained with DAPI for microscopy at 30 hpi. DAPI (blue), Clover  
257 (green). Arrow indicates the position of the chlamydial inclusion. Size bar = 10  $\mu$ m.  
258

259 To determine the effects of theophylline and gene expression induction on  
260 chlamydial growth dynamics the production of infectious EBs using a reinfection inclusion  
261 forming unit assay was performed. Cos-7 cells were infected with L2-E-clover-flag and  
262 induced with theophylline at 16 hpi. EBs were harvested at 30 hpi and 48 hpi. Clover  
263 induction with theophylline had no significant effect on EB production at 30 hpi  
264 (supplemental S1) or 48 hpi (Fig. 2A). The control of expression of ectopic proteins to  
265 assess their function in pathogenesis needs to be highly customizable as too little or too  
266 high concentrations may mask the phenotype of interest. Therefore we assessed the  
267 dose responsiveness of the E riboswitch to its ligand theophylline. Gene expression was  
268 measured using live-cell time-lapse microscopy and particle tracking to quantify the  
269 fluorescent expression of individual inclusions over time [22,23]. This technique allows  
270 for the tracking of gene expression in multiple individual inclusions over the entire  
271 developmental cycle. Cos-7 cells were plated in a glass bottom 24 well plate and infected  
272 with L2-E-clover-flag at an multiplicity of infection (MOI) of ~0.5. At 16 hpi theophylline at  
273 1mM, 0.5 mM, 0.25mM, 0.0125 mM, 0.00625 mM, and 0.00312 mM was added to  
274 individual wells to induce Clover expression; images were taken every 15 minutes for 48  
275 hours. Clover expression followed a dose response with almost immediate detection of  
276 fluorescence with 1mM theophylline and a delayed response at the lowest dose, 0.00312  
277 mM (Fig. 2B). The response increased through the life of the inclusion; this increase  
278 overtime also followed a dose response (Fig. 2B)  
279

280 **Figure 2. Characterization of p2TK2-SW2-T5-E-clover-flag.** A) Cos-7 cells were  
281 infected with L2-T5-E-clover-flag and the production of infectious progeny was  
282 determined at 48 hpi after 0.5 mM theophylline induction or vehicle only. B) Cos-7 cells  
283 were infected with L2-T5-E-clover-flag, treated with varying dilutions of theophylline at 16  
284 hpi (1 mM, 0.5 mM, 0.25 mM, 0.125 mM, 0.0625 mM, 0.03125mM) and imaged for 50  
285 hours using live cell imaging. The Clover expression intensities from >50 individual  
286 inclusions were monitored via automated live-cell fluorescence microscopy and average  
287 intensities were plotted. Live cell imaging demonstrated that Clover induction was dose



288 responsive. Cloud represents SEM. Y-axes are denoted in scientific notation. Error bars  
289 = SEM.

290

## 291 **Translational control of gene expression from a native chlamydial** 292 **promoter.**

293 The use of non endogenous promoters for ectopic expression is an important tool  
294 for understanding protein function. However, these systems lack the ability to control gene  
295 expression through native gene regulation making it difficult to modulate expression at  
296 biologically relevant times or in the correct cell subspecies. This is especially true for  
297 *Chlamydia* as it proceeds through a time dependent developmental cycle that includes  
298 multiple phenotypic cell types. Therefore, the use of translational control was tested in  
299 concert with a native chlamydial promoter. We tested the effectiveness of translational  
300 control on the *pgp4* native plasmid gene. *Pgp4* is a regulator of other plasmid genes as  
301 well as chromosomal genes [24–26]. *Ctr* strains with *pgp4* knocked out from the native  
302 plasmid show marked changes in gene expression and a phenotypic loss of glycogen  
303 accumulation [26]. To assess the ability to regulate translation of transcripts from a native  
304 promoter, the E riboswitch was cloned upstream of the *pgp4* open reading frame (ORF)  
305 replacing the predicted ribosome binding site (Fig. 3A). The insertion was designed to not  
306 disrupt the native promoter region of *pgp4*. A flag tag was also added in frame to the end  
307 of the *pgp4* ORF creating the plasmid p2TK2-SW2-nprom-E-*pgp4*-3xflag (Fig 3A). This  
308 plasmid was then transformed into *Ctr* L2 to create L2-nprom-E-*pgp4*-flag. To assess  
309 expression, Cos-7 cells were infected with the L2-nprom-E-*pgp4*-flag strain in the  
310 presence of 0.5 mM theophylline. Expression was assessed by western blotting and the  
311 flag tag was only detectable in theophylline treated samples. The control of *pgp4*  
312 expression was also assessed by confocal microscopy. Cos-7 cells were plated on  
313 coverslips and infected with L2-nprom-E-*pgp4*-flag and treated with 0.5 mM theophylline  
314 at infection. The coverslips were fixed at 30 hpi, stained with an anti-flag antibody and  
315 DAPI for visualization (Fig. 3C). Like for the western blotting experiment, the flag epitope  
316 was only detected in the theophylline induced samples (Fig 3C). The effect of modulating  
317 *pgp4* expression on EB production was determined using a re-infection assay. Cos-7 cells  
318 were infected with L2-nprom-E-*pgp4*-flag and translation was induced at infection with 0.5  
319 mM theophylline. EBs were harvested at 48 hours and monolayers were re-infected and  
320 inclusions quantified. Repression of *pgp4* expression resulted in a slight but statistically  
321 significant increase in infectious progeny as compared to induced *pgp4* expression (Fig.  
322 3D). *Pgp4* positively regulates the expression of *GlgA* which is involved in accumulation  
323 of glycogen in the inclusion. When *pgp4* expression is missing the *Ctr* inclusion does not  
324 accumulate glycogen and is phenotypically similar to the plasmidless L2 strain, L2R [26].  
325 Therefore, we tested the ability of translational regulation to control glycogen  
326 accumulation in the inclusion. Cos-7 cells were infected with the L2-nprom-E-*pgp4*-flag  
327 strain and treated or not with 0.5 mM theophylline at the time of infection. Cells were

328 stained for glycogen accumulation at 36 hpi using Lugol's iodine solution as previously  
329 described [26]. As expected from the flag detection of expression, glycogen staining was  
330 only evident in inclusions that were treated with theophylline (Fig. 3E). The uninduced  
331 inclusions were morphology similar to inclusions formed by the plasmidless strain L2R  
332 which lack glycogen accumulation (Fig. 3E).

333  
334 **Figure 3. Characterization of p2TK2-SW2-nprom-E-pgp4-flag.** A) Schematic of the  
335 nprom-E-pgp4-flag construct consisting of the native pgp4 promoter, the riboE riboswitch  
336 (rsE), and the pgp4 ORF with an inframe 3x flag tag. B) Anti-flag western blot of Cos-7  
337 cells infected with L2-nprom-E-pgp4-flag comparing expression of theophylline treated  
338 and untreated cultures. Cells were induced or not with 0.5mM theophylline at 16 hpi and  
339 proteins were harvested at 30 hpi. C) Confocal micrographs of Cos-7 cells infected with  
340 L2-nprom-E-pgp4-flag, induced or not with 0.5 mM theophylline at 16 hpi and fixed and  
341 stained with DAPI to detect DNA. The flag tag was detected using a primary antibody to  
342 the tag and an alexa 488 anti-mouse secondary antibody (green). Size bar = 10  $\mu$ m. D)  
343 Cos-7 cells were infected with L2-nprom-E-pgp4-flag and the production of infectious  
344 progeny was determined at 48 hpi after 0.5 mM theophylline induction or vehicle only. E)  
345 Iodine staining of glycogen in the inclusion of Cos-7 cells infected with L2-nprom-E-pgp4-  
346 flag after 0.5 mM theophylline induction at 16 hpi or vehicle only. Arrows indicate the  
347 location of the chlamydial inclusions. Asterisk denotes p-value < 0.05. Error bars = SEM.

348  
349 **Transcriptional and translational control of gene expression.**

350 The E riboswitch partnered with either the T5 promoter or native pgp4 promoter  
351 offered very tight expression control. There was no detectable Clover or Pgp4 by western  
352 blotting and no fluorescence from Clover or Flag staining detected using confocal  
353 microscopy (Fig. 1 and 3). However, we attempted to use the T5-E system to ectopically  
354 express the *Chlamydia* histone like protein HctB. Clover was replaced on the p2TK2-  
355 SW2-T5-E-clover-3xflag plasmid with HctB creating p2TK2-SW2-T5-E-hctB-3xflag. This  
356 construct was then transformed into *Ctr*. Although we successfully isolated transformants,  
357 when the plasmids were purified and sequenced, the promoter region of the plasmid was  
358 mutated in every case. Additionally the transformants did not produce HctB as assayed  
359 by western blotting for the flag tag (Data not shown). We reasoned that the HctB protein  
360 expression was leaky enough to lead to small amounts of HctB accumulation despite the  
361 translation inhibition of the E riboswitch, thereby inhibiting the chlamydial developmental  
362 cycle. We therefore sought to create an extremely tightly regulated inducible expression  
363 system by combining inducible transcription with inducible translation. For this construct  
364 we added the Tet repressor and replaced the T5 promoter with a Tet promoter containing  
365 Tet operator sites in the p2TK2-SW2-T5-E-clover-3xflag plasmid [27] (Fig. 4A). In addition  
366 to replacing the T5 promoter with the Tet promoter, a ribozyme insulator was added to  
367 the E riboswitch to decouple the promoter from the riboswitch (Fig. 4A). The riboJ

368 ribozyme insulator is a self cleaving 75 nucleotide sequence from the satellite RNA of  
369 tobacco ringspot virus (sTRSV) followed by a 23 nucleotide hairpin [28]. After  
370 transcription, the ribozyme self-cleaved, removing upstream sequences, eliminating the  
371 promoter-associated RNA leader (Fig. S2). This resulted in transcripts with a small hairpin  
372 region just upstream of the E riboswitch that we hypothesized would not affect the  
373 aptamer function of the riboswitch. We used this same regulatory scheme to control the  
374 expression of both Clover and HctB resulting in plasmids p2TK2-SW2-Tet-J-E-clover-  
375 3xflag and p2TK2-SW2-Tet-J-E-hctB-3xflag. For the HctB clone we used the AUG start  
376 site and the first three codons of the Clover gene followed by the HctB ORF without the  
377 AUG. We chose to use the first 3 codons of Clover as some genes in *Chlamydia* have  
378 small RNA regulatory sites at the beginning of the gene and wanted to avoid any native  
379 regulation [29]. These constructs were transformed into *Ctr* creating the strains L2-Tet-J-  
380 E-clover-flag and L2-Tet-J-E-hctB-flag.

381  
382 **Figure 4. Characterization of p2TK2-SW2-Tetp-riboJ-E-clover-flag.** A) Schematic of  
383 the Tet-riboJ-E-clover-flag construct consisting of the tet repressor, tet promoter, riboJ  
384 insulator, riboE riboswitch (rsE) and the ORF for the clover fluorescent protein containing  
385 an inframe 3x flag tag. B) Anti-flag western blot of Cos-7 cells infected with L2-Tet-J-E-  
386 clover-flag comparing expression of theophylline treated and untreated cultures. Cells  
387 were induced with 0.5 mM theophylline, 30ng/ml aTc, both aTc and theophylline or vehicle  
388 only at 16 hpi and proteins were harvested at 30 hpi. C) Confocal micrographs of Cos-7  
389 cells infected with L2-Tet-J-E-clover-flag, induced with 0.5 mM theophylline, 30ng/ml aTc,  
390 both aTc and theophylline or vehicle only at 16 hpi and fixed and stained with DAPI (blue)  
391 for confocal microscopy at 30 hpi. Clover expression (green) was evident in cells treated  
392 with aTc and Theophylline. Size bar = 10  $\mu$ m. D) Cos-7 cells were infected with L2-Tet-  
393 J-E-clover-flag and the production of infectious progeny was determined at 48 hpi after  
394 induction with 0.5 mM theophylline, 30ng/ml aTc, both aTc and theophylline or vehicle  
395 only at 16 hpi. Production of infectious progeny was determined using a reinfection assay.  
396 Asterisk denotes p-value < 0.05. Error bars = SEM.

397  
398 Expression of Clover from p2TK2-SW2-Tet-J-E-clover-3xflag was evaluated by  
399 western blotting. Cos-7 cells were infected with the L2-Tet-J-E-clover-flag strain and  
400 expression was induced with the addition of either anhydroTetracycline (aTc) 30ng/ml or  
401 theophylline 0.5 mM alone, or both combined at 16 hpi. At 30 hpi protein from the infected  
402 cells was harvested, separated by PAGE and blotted to nitrocellulose for detection. Clover  
403 expression was detected using an anti-flag antibody. As expected Clover expression was  
404 only detected in samples induced with both aTc and theophylline (Fig. 4B). We also  
405 evaluated Clover expression using confocal microscopy. Cos-7 cells plated on glass  
406 coverslips were infected for 16 hours before induction of expression with aTc 30ng/ml,  
407 theophylline 0.5 mM or both combined. The coverslips were fixed at 30 hpi, stained with

408 DAPI and visualized by confocal microscopy. Again, robust Clover expression was only  
409 evident when both transcription and translation were induced (Fig. 4C).

410 The effects of induction of this system was evaluated for effects on the chlamydial  
411 developmental cycle. The impact of induction on the production of infectious EBs was  
412 measured using an inclusion forming reinfection assay (IFU). Cos-7 cells were infected  
413 with L2-Tet-J-E-clover-flag and Clover expression was induced with aTc 30ng/ml,  
414 theophylline 0.5 mM or both combined at 16 hpi. EBs were harvested at both 30 hpi and  
415 48 hpi to evaluate the production of infectious progeny (Fig. 4D and S1). Each inducer  
416 alone had no effect on IFU formation. However, the addition of both inducers had a very  
417 small but statistically significant reduction in IFUs suggesting the expression of Clover  
418 resulted in a slight impact to the chlamydial developmental cycle (Fig. 4D and S1).

419 To assess the effects of the induction of transcription or translation order we  
420 measured the kinetics of Clover expression using live cell imaging as described earlier.  
421 Cos-7 cells plated into 24 well glass bottom plates were infected with L2-Tet-J-E-clover-  
422 flag and either treated with aTc (30ng/ml) at infection and treated with a decreasing dose  
423 of theophylline (2 fold dilutions from 1 mM to 0.0312 mM) at 16 hpi (Fig. 5A) or  
424 theophylline (0.5 mM) at infection followed by a decreasing dose of aTc (2 fold dilutions  
425 from 60 ng/ml to 1.25 ng/ml) at 16 hpi (Fig. 5B). Infected cells were imaged for Clover  
426 expression every 30 minutes for 50 hours. Gene expression was quantified using live-cell  
427 time-lapse microscopy and particle tracking to quantify the fluorescent expression of  
428 individual inclusions over time [23]. Clover expression using transcriptional induction  
429 followed by translational induction demonstrated a robust dose response. Expression was  
430 detectable almost immediately after theophylline addition and detected at the lowest dose  
431 of 0.0312 mM theophylline (Fig. 5A). Interestingly, max expression kinetics was observed  
432 with 0.5 mM of theophylline while 1 mM resulted in less expression suggesting potential  
433 toxicity at high concentrations (Fig. 5A). When transcription was induced first (aTc)  
434 followed by translational induction at 16 hpi, expression was again initiated with little delay  
435 and a very strong dose response was observed (Fig. 5B). Transcriptional induction with  
436 aTc resulted in higher expression as we did not reach a point of toxicity. This resulted in  
437 the highest expression being at the highest concentration of aTc (60 ng/ml) (Fig. 5B). No  
438 induction was observed at the lowest aTc concentration (1.25 ng/ml). Notably,  
439 transcriptional induction followed by translational induction resulted in slightly higher  
440 induction as compared to translational induction followed by transcriptional induction as  
441 can be seen by comparing aTc 30 ng/ml followed by 0.5 mM theophylline at 16 hpi to 0.5  
442 mM theophylline at infection followed by 30 ng/ml of aTc at 16 hpi (Fig. 5A and B).

443  
444 **Figure 5. Induction kinetics of p2TK2-SW2-Tet-J-E-clover-flag.** A) Cos-7 cells were  
445 infected with L2-Tet-J-E-clover-flag, treated with varying dilutions of theophylline at 16 hpi  
446 (1 mM, 0.5 mM, 0.25 mM, 0.125 mM, 0.0625 mM, 0.03125mM) and 30 ng/ml aTc at 0  
447 hpi. The infections were monitored using live cell imaging for 50 hours. B) Cos-7 cells

448 were infected with L2-Tet-riboJ-E-clover-flag, treated with varying dilutions of aTc at 16  
449 hpi (60 ng/ml, 30 ng/ml, 15 ng/ml, 7.5 ng/ml, 3.75 ng/ml, 1.875 ng/ml) and 0.5 mM  
450 theophylline at 0 hpi. The infections were monitored using live cell imaging for 50 hours.  
451 Expression intensities from >50 individual inclusions were monitored via automated live-  
452 cell fluorescence microscopy and the mean intensities are shown. Cloud represents SEM.  
453 Y-axes are denoted in scientific notation.

454

455 To test the effective repression of gene expression of this system p2TK2-SW2-  
456 Tet-J-E-hctB-3xflag (Fig. 6A) was transformed into *Ctr* producing L2-Tet-J-E-hctB-flag.  
457 Unlike the p2TK2-SW2-E-hctB-3xflag construct, p2TK2-SW2-Tet-J-E-hctB-3xflag  
458 successfully transformed into *Ctr* without accumulating mutations suggesting tighter  
459 repression of leaky expression. Cos-7 cells were infected with L2-Tet-J-E-hctB-flag and  
460 induced for HctB expression with 30 ng/ml aTc and 0.5 mM theophylline at 16 hpi. Protein  
461 was isolated, separated by PAGE, blotted to nitrocellulose and expression was evaluated  
462 using an anti-flag antibody. HctB-flag was detected only when both inducers (aTc and  
463 theophylline) were used (Fig. 6B). Gene expression was also assessed using confocal  
464 microscopy. Cos-7 cells were plated onto glass coverslips and infected with L2-Tet-J-E-  
465 hctB-flag. Gene expression was induced with 30 ng/ml aTc, 0.5 mM theophylline, or both  
466 at 16 hpi and the coverslips were fixed and stained with an anti-flag antibody at 30 hpi  
467 before mounting for confocal microscopy. Confocal microscopy confirmed HctB induction  
468 with both the transcription and translation inducer added (Fig. 6C). However, HctB  
469 expression was detected at low levels when induced with aTc only suggesting  
470 translational repression with this construct was slightly leaky (Fig. 5C).

471 As we could not transform p2TK2-SW2-T5-E-hctB-flag into *Chlamydia*, we  
472 hypothesized that expression of HctB inhibited the formation of the infectious EB cell form.  
473 To test this, Cos-7 cells were infected with L2-Tet-J-E-hctB-flag and induced with 30 ng/ml  
474 aTc, 0.5 mM theophylline, or both at 16 hpi and EBs were harvested at 30 hpi and 48 hpi.  
475 Induction of both transcription and translation resulted in a greater than 2.5 log reduction  
476 in infectious progeny at both 30 hpi and 48 hpi (Fig 6D, S1). Confocal microscopy  
477 indicated that transcription induction with aTc only resulted in low but detectable HctB  
478 production (Fig. 5C) and this leaky expression was also evident when assaying for  
479 infectious progeny. Induction of transcription only resulted in about a log reduction in  
480 infectious progeny at both 30 hpi and 48 hpi (Fig. 6D, S1). Translation induction only  
481 resulted in a slight but statistically significant decrease in EB production as compared to  
482 no induction control (Fig 6D, S1). Together these data suggest that the combination of  
483 transcriptional repression and translational inducible regulation was significantly tight  
484 enabling *Chlamydia* to be successfully transformed with the construct and that induction  
485 was sufficiently high to induce the inhibition of the production of infectious progeny.

486



487 **Figure 6. Characterization of p2TK2-SW2-Tet-J-E-hctB-flag.** A) Schematic of the Te-  
488 riboJ-E-hctB-flag construct. HctB expression is controlled by an aTc inducible promoter,  
489 riboJ insulator and the riboE riboswitch. B) Anti-flag western blot of Cos-7 cells infected  
490 with L2-Tet-J-E-hctB-flag comparing expression of theophylline treated and untreated  
491 cultures. Cells were induced with 0.5 mM theophylline, 30ng/ml aTc, both aTc and  
492 theophylline or vehicle only at 16 hpi and proteins were harvested at 30 hpi. HctB-flag  
493 expression was only detected in the samples induced with both aTc and theophylline. C)  
494 Confocal micrographs of Cos-7 cells infected with L2-Tet-riboJ-E-hctB-flag, induced with  
495 0.5 mM theophylline, 30ng/ml aTc, both aTc and theophylline or vehicle only at 16 hpi  
496 and fixed and stained with DAPI (blue) for confocal microscopy at 30 hpi. The flag tag  
497 was stained with a primary antibody to the flag and an alexa 488 anti-mouse secondary  
498 antibody (green). Size bar = 10  $\mu$ m. D) Production of infectious progeny was determined  
499 using a reinfection assay. Cos-7 cells were infected with L2-Tet-J-E-hctB-flag and the  
500 production of infectious progeny was determined at 48 hpi after induction with 0.5 mM  
501 theophylline, 30ng/ml aTc, both aTc and theophylline or vehicle only at 16 hpi. Asterisks  
502 denote p-values < 0.05. Error bars = SEM.

503

#### 504 **Expression from T5 and Tet-J-E is cell type specific.**

505 Chlamydial infection of vertebrate cells consists of a multiple cell type  
506 developmental cycle. For *Ctr* L2 the elementary body (EB) cell type mediates cell entry  
507 and differentiates into the reticulate body (RB) cell type over an ~10 hour period before  
508 initiating cell division. The RB cell type undergoes growth and division leading to an  
509 expansion of RB numbers. The RB cell type also matures during this process eventually  
510 producing an intermediate body (IB) cell type that matures back into the EB cell form over  
511 ~8 hours [23]. Our studies have shown that different promoters are active in these distinct  
512 cell populations [23]. Confocal microscopy of Clover expression and flag staining for both  
513 the T5-E-clover-flag and Tet-J-E-clover-flag constructs appeared non uniform in the  
514 inclusion suggesting expression in only a subset of cells. To determine the cells in which  
515 these promoters were active we replaced Clover in both of these constructs with the GFP  
516 variant Neongreen and added an inframe LVA degradation tag to produce the plasmids  
517 p2TK2-SW2-T5-E-ngLVA-3xFlag and p2TK2-SW2-Tet-J-E-ngLVA-3xFlag. Neongreen-  
518 LVA (ngLVA) protein had a halflife of ~ 20 minutes in *Chlamydia* (data not shown). The  
519 plasmids were transformed into *Chlamydia* and the expression pattern of these constructs  
520 was compared to that of p2TK2-SW2-euoprom-ngLVA. p2TK2-SW2-euoprom-ngLVA,  
521 like p2TK2-SW2-euoprom-Clover [23] uses the euo promoter to drive expression  
522 specifically in the RB cell type. Cos-7 cells infected with L2 T5-E-ngLVA, L2 Tet-J-E-  
523 ngLVA, or L2 euoprom-ngLVA were fixed for confocal microscopy at 30 hpi. Expression  
524 of ngLVA for all three promoters was very similar showing expression in a subset of large  
525 cells suggestive of RBs (Fig 7A). Quantification of the number of cells per inclusion that  
526 expressed ngLVA from each promoter showed that all three promoters expressed ngLVA



527 in similar numbers of cells. This suggests that both of the synthetic sigma70 optimized  
528 promoters (T5 and Tet) when used in *Chlamydia* expressed primarily in the RB cell type  
529 and not in the IB.

530

531 **Figure 7. Promoter cell type expression.** A) Confocal micrographs of Cos-7 cells  
532 infected with L2-euo-neogreenLVA (euo-ngLVA), L2-T5-E-neogreenLVA (T5-E-ngLVA),  
533 or L2-Tet-J-E-neogreenLVA (Tet-E-ngLVA) (green) and fixed and stained with DAPI  
534 (blue) at 30 hpi. Size bar = 10  $\mu$ m. B) Quantification of > 20 neogreenLVA expressing  
535 chlamydial cells for each promoter construct. Error bars = SEM.

536

537

## 538 **Discussion:**

539 Ectopic gene expression is an important tool for uncovering the function of potential  
540 virulence associated genes in pathogenic bacteria. We have adapted the E riboswitch, a  
541 theophylline binding aptamer, to regulate gene translation in *Chlamydia trachomatis*.  
542 Riboswitches have been used in many organisms to regulate gene expression [14–  
543 16,30–32]. In bacteria, riboswitches are constructed of aptamers that fold to block  
544 ribosome assembly at the translational start site in the absence of their cognate ligand.  
545 This translational control can be combined with strong synthetic promoters, native  
546 promoters, cell type specific promoters, temporal promoters or inducible promoters to add  
547 increasingly granular expression control of effectors and regulatory proteins. In this study  
548 we combined the E riboswitch with the strong synthetic promoter T5 and demonstrated  
549 that the riboswitch efficiently repressed translation of Clover and was strongly inducible  
550 by theophylline. In addition this induction was dose responsive providing an excellent tool  
551 for the control of ectopic gene expression. In addition to combining translational  
552 expression control with a strong promoter, we also demonstrated that it can be used with  
553 a native chlamydial promoter. The E riboswitch was cloned upstream of the ORF for the  
554 plasmid gene *pgp4*. Pgp4 is a gene expression regulator for both chromosomal and  
555 plasmids genes and the absence of *pgp4* results in a loss of glycogen accumulation in  
556 the inclusion [26]. The addition of the E riboswitch led to undetectable levels of Pgp4  
557 expression and the loss of glycogen accumulation when theophylline was absent. The  
558 addition of theophylline during infection restored functional levels of Pgp4 as  
559 demonstrated by the restoration of glycogen accumulation in the inclusion and detectable  
560 expression of Pgp4 via western blot and confocal microscopy.

561 By combining translational control with transcriptional control we were able to  
562 improve the repression of protein expression. The T5 promoter-E-riboswitch combination  
563 proved to have undetectable expression when driving Clover expression as assessed by  
564 western blotting and confocal microscopy. However, when attempting to express the  
565 chlamydial protein HctB, a protein involved in controlling the developmental cycle, leaky  
566 expression resulted in mutation of the plasmid causing HctB to not express. By combining

567 translational control (E riboswitch) with transcription control (Tet inducible promoter), we  
568 created an extremely tightly regulated gene expression system. The E riboswitch requires  
569 the 5'-UTR of the transcript to properly fold and block the ribosome binding site of the  
570 transcript. Combining the E riboswitch with different promoters and different transcription  
571 start sites can potentially affect the folding of the riboswitch, thus changing its repression  
572 and induction properties. To eliminate this effect and increase the reliability of the  
573 riboswitch in relation to a variety of promoters, we cloned the riboJ ribozyme insulator  
574 upstream of the E riboswitch. The riboJ insulator is made up of the sTRSV-ribozyme with  
575 an additional 23-nt hairpin immediately downstream [28,33,34]. This hairpin imposes  
576 structure to the UTR just upstream of the E riboswitch, minimizing its influence on the  
577 folding of the riboswitch and ensuring any upstream structure is consistent between  
578 promoters.

579 Surprisingly, the order of induction (transcription vs translation) did not significantly  
580 change the gene expression kinetics suggesting that there was not an accumulation of  
581 transcripts after Tet induction that then could be induced to initiate translation. Instead,  
582 this observation suggests the transcripts either don't accumulate or, after folding into the  
583 inhibited structure in the absence of theophylline they don't then refold revealing the RBS  
584 upon theophylline addition. This suggests theophylline binding competes with inhibitory  
585 folding during mRNA synthesis.

586 HctB, when cloned into this dual induction plasmid was successfully transformed  
587 into *Chlamydia* and was inducible with the addition of both theophylline and aTc as  
588 detected by western blotting and confocal microscopy. Additionally, ectopic expression of  
589 HctB early in infection (16 hpi) inhibited the formation of infectious progeny. Together,  
590 these data confirm that leaky expression from T5-E likely rendered successful  
591 transformation of this clone impossible. Therefore, the combination of transcriptional and  
592 translational control is an ideal system to study the effects of toxic proteins or proteins  
593 that regulate the developmental cycle.

594 Interestingly, both the T5-E and Tet-riboJ-E promoter systems appear to only  
595 significantly express in the RB cell type. The promoters for both of these constructs are  
596 based on *E. coli* sigma70 consensus sequences and are constitutive in many bacteria  
597 [35,36]. In *Chlamydia* these promoters appear to express primarily in the RB cell type  
598 suggesting gene expression in the intermediate body (IB) and EB cell type may require  
599 specific promoters or additional regulatory elements. Our data suggest that the ability to  
600 add translational control independently from transcriptional control using riboJ ribozyme  
601 and E riboswitch will be an important tool in controlling ectopic gene expression in these  
602 chlamydial cell types.

603 Adding inducible translational control to the tool box for chlamydial genetic tools  
604 increases opportunities to unveil the function of *Chlamydia* regulatory genes and effector  
605 genes to reveal their role in pathogenesis. The ability to control the timing and strength of

606 gene expression independently from promoter strength and timing increases the utility of  
607 ectopic gene expression and provides an important tool for studying chlamydial  
608 pathogenesis.

609

## 610 **Acknowledgments:**

611 We would like to thank Dr. Paul Beare at the Rocky Mountain Labs for providing us the  
612 Tet repressor and promoter sequence. We would also like to thanks Dr. John-Demian  
613 (JD) Sauer for providing us with the T5prom-E promoter and riboswitch.

614

## 615 **References:**

- 616 1. Owusu-Edusei KJ, Chesson HW, Gift TL, Tao G, Mahajan R, Ocfemia MCB, et al.  
617 The Estimated Direct Medical Cost of Selected Sexually Transmitted Infections in  
618 the United States, 2008. *Sex Transm Dis.* 2011;40: 197201.  
619 doi:10.1097/OLQ.0b013e318285c6d2
- 620 2. Owusu-Edusei K, Roby TM, Chesson HW, Gift TL. Productivity costs of nonviral  
621 sexually transmissible infections among patients who miss work to seek medical  
622 care: evidence from claims data. *Sex Health.* CSIRO PUBLISHING; 2011;10:  
623 434437. doi:10.1071/SH13021
- 624 3. Torrone EA, Bernstein KT. Surveillance for Sexually Transmitted Diseases.  
625 Concepts and Methods in Infectious Disease Surveillance. John Wiley & Sons, Ltd;  
626 2014. pp. 122131. doi:10.1002/9781118928646.ch12
- 627 4. Bbar C, de Barbeyrac B. Genital Chlamydia trachomatis infections. *Clin Microbiol*  
628 *Infect Off Publ Eur Soc Clin Microbiol Infect Dis.* 15: 410. doi:10.1111/j.1469-  
629 0691.2008.02647.x
- 630 5. Ohman H, Tiitinen A, Halttunen M, Lehtinen M, Paavonen J, Surcel H-M. Cytokine  
631 polymorphisms and severity of tubal damage in women with Chlamydia-associated  
632 infertility. *J Infect Dis.* 199: 13531359. doi:10.1086/597620
- 633 6. Miller WC, Ford CA, Morris M, Handcock MS, Schmitz JL, Hobbs MM, et al.  
634 Prevalence of chlamydial and gonococcal infections among young adults in the  
635 United States. *JAMA: J Am Med Assoc.* 291: 22292236.  
636 doi:10.1001/jama.291.18.2229
- 637 7. Datta SD, Torrone E, Kruszon-Moran D, Berman S, Johnson R, Satterwhite CL, et  
638 al. Chlamydia trachomatis trends in the United States among persons 14 to 39  
639 years of age, 1999-2008. *Sex Transm Dis.* 39: 9296.  
640 doi:10.1097/OLQ.0b013e31823e2ff7
- 641 8. Bebear C, Barbeyrac BD. Genital Chlamydia trachomatis infections. *Clinical*  
642 *Microbiology and Infection.* Elsevier; 2009. pp. 410. doi:10.2471/BLT.18.228486
- 643 9. Brothwell JA, Muramatsu MK, Zhong G, Nelson DE. Advances and Obstacles in the  
644 Genetic Dissection of Chlamydial Virulence. *Current Topics in Microbiology and*  
645 *Immunology.* Springer Nature; 2018. pp. 133158. doi:10.1007/82\_2017\_76
- 646 10. Rahnama M, Fields KA. Transformation of Chlamydia: current approaches and  
647 impact on our understanding of chlamydial infection biology. *Microbes and*

- 648 Infection. Elsevier; 2018. pp. 445450. doi:10.1016/J.MICINF.2018.01.002
- 649 11. Thomson NR, Clarke IN. Chlamydia trachomatis: small genome, big challenges.  
650 Future Microbiology. Future Medicine; 2010. pp. 55561. doi:10.2217/FMB.10.31
- 651 12. Breaker RR. Prospects for riboswitch discovery and analysis. Molecular Cell.  
652 Elsevier; 2011. pp. 86779. doi:10.1016/J.MOLCEL.2011.08.024
- 653 13. Lynch SA, Gallivan JP. A flow cytometry-based screen for synthetic riboswitches.  
654 Nucleic Acids Research. Oxford University Press; 2008. pp. 18492.  
655 doi:10.1093/NAR/GKN924
- 656 14. Vlack ERV, Seeliger JC. Using riboswitches to regulate gene expression and define  
657 gene function in mycobacteria. Methods in Enzymology. Elsevier; 2014. pp.  
658 25165. doi:10.1016/BS.MIE.2014.10.034
- 659 15. Rudolph MM, Vockenhuber MP, Suess B. Conditional control of gene expression by  
660 synthetic riboswitches in *Streptomyces coelicolor*. Methods in Enzymology.  
661 Elsevier; 2014. pp. 28399. doi:10.1016/BS.MIE.2014.10.036
- 662 16. Topp S, Reynoso CMK, Seeliger JC, Goldlust IS, Desai SK, Murat D, et al.  
663 Synthetic riboswitches that induce gene expression in diverse bacterial species.  
664 Appl Environ Microbiol. Department of Chemistry, Center for Fundamental and  
665 Applied Molecular Evolution, Emory University, Atlanta, GA 30322, USA.: American  
666 Society for Microbiology; 2008;76: 78817884. doi:10.1128/AEM.01537-10
- 667 17. Bryksin AV, Matsumura I. Rational design of a plasmid origin that replicates  
668 efficiently in both gram-positive and gram-negative bacteria. PLoS ONE. Public  
669 Library of Science; 2010. doi:10.1371/JOURNAL.PONE.0013244
- 670 18. Gentz R, Bujard H. Promoters recognized by *Escherichia coli* RNA polymerase  
671 selected by function: highly efficient promoters from bacteriophage T5. Journal of  
672 Bacteriology. American Society for Microbiology; 1985. pp. 707.  
673 doi:10.1128/JB.164.1.70-77.1985
- 674 19. Cui W, Han L, Cheng J, Liu Z, Zhou L, Guo J, et al. Engineering an inducible gene  
675 expression system for *Bacillus subtilis* from a strong constitutive promoter and a  
676 theophylline-activated synthetic riboswitch. Microbial Cell Factories. Springer  
677 Nature; 2016. doi:10.1186/S12934-016-0599-Z
- 678 20. Agaisse H, Derr I. A *C. trachomatis* cloning vector and the generation of *C.*  
679 *trachomatis* strains expressing fluorescent proteins under the control of a *C.*  
680 *trachomatis* promoter. PLoS ONE. Public Library of Science; 2013.  
681 doi:10.1371/JOURNAL.PONE.0057090
- 682 21. Wang Y, Kahane S, Cutcliffe LT, Skilton RJ, Lambden PR, Clarke IN. Development  
683 of a Transformation System for *Chlamydia trachomatis*: Restoration of Glycogen  
684 Biosynthesis by Acquisition of a Plasmid Shuttle Vector. PLoS Pathog. Public  
685 Library of Science; 2011;7: 1002258. Available:  
686 <http://dx.plos.org/10.1371/journal.ppat.1002258>
- 687 22. Chiarelli TJ, Grieshaber NA, Grieshaber SS. Live-Cell Forward Genetic Approach to  
688 Identify and Isolate Developmental Mutants in *Chlamydia trachomatis* JoVE.  
689 MyJoVE Corp; 2020. p. e61365. doi:10.3791/61365
- 690 23. Chiarelli TJ, Grieshaber NA, Omsland A, Remien CH, Grieshaber SS. Single  
691 Inclusion Kinetics of *Chlamydia trachomatis* Development. mSystems.00689-20.  
692 mSystems. 2020. doi:10.1128/mSystems.00689-20

- 693 24. Zhang Q, Rosario CJ, Sheehan LM, Rizvi SM, Brothwell JA, He C, et al. The  
694 Repressor Function of the Chlamydia Late Regulator EUO Is Enhanced by the  
695 Plasmid-Encoded Protein Pgp4. *Journal of Bacteriology*. American Society for  
696 Microbiology; 2020. doi:10.1128/JB.00793-19
- 697 25. Gong S, Yang Z, Lei L, Shen L, Zhong G. Characterization of Chlamydia  
698 trachomatis Plasmid-Encoded Open Reading Frames. *J Bacteriol*. 195: 38193826.  
699 doi:10.1128/JB.00511-13
- 700 26. Song L, Carlson JH, Whitmire WM, Kari L, Virtaneva K, Sturdevant DE, et al.  
701 Chlamydia trachomatis plasmid-encoded Pgp4 is a transcriptional regulator of  
702 virulence-associated genes. *Infect Immun*. 81: 636644. doi:10.1128/IAI.01305-12
- 703 27. Beare PA, Gilk SD, Larson CL, Hill J, Stead CM, Omsland A, et al. Dot/Icm type IVB  
704 secretion system requirements for Coxiella burnetii growth in human macrophages.  
705 *MBio*. American Society for Microbiology; 2011. pp. e00175-11.  
706 doi:10.1128/MBIO.00175-11
- 707 28. Clifton KP, Jones EM, Paudel S, Marken JP, Monette CE, Halleran AD, et al. The  
708 genetic insulator RiboJ increases expression of insulated genes. *Journal of*  
709 *Biological Engineering*. Springer Nature; 2018. doi:10.1186/S13036-018-0115-6
- 710 29. Grieshaber NA, Tattersall JS, Liguori J, Lipat JN, Runac J, Grieshaber SS.  
711 Identification of the base-pairing requirements for repression of hctA translation by  
712 the small RNA IhtA leads to the discovery of a new mRNA target in Chlamydia  
713 trachomatis. *PloS one*. Public Library of Science; 2013;10: e0116593.  
714 doi:10.1371/journal.pone.0116593
- 715 30. Lease RA. Riboregulation in Escherichia coli: DsrA RNA acts by RNA:RNA  
716 interactions at multiple loci. *Proc Natl Acad Sci*. 1996;95: 1245612461.  
717 doi:10.1073/pnas.95.21.12456
- 718 31. Reynoso CMK, Miller MA, Bina JE, Gallivan JP, Weiss DS. Riboswitches for  
719 intracellular study of genes involved in Francisella pathogenesis. *mBio*. Department  
720 of Chemistry, Emory University, Atlanta, Georgia, USA.: American Society for  
721 Microbiology; 2010;3: e00253-12. doi:10.1128/mBio.00253-12
- 722 32. Nakahira Y, Ogawa A, Asano H, Oyama T, Tozawa Y. Theophylline-dependent  
723 riboswitch as a novel genetic tool for strict regulation of protein expression in  
724 Cyanobacterium Synechococcus elongatus PCC 7942. *Plant & cell Physiol*.  
725 54: 17241735. doi:10.1093/pcp/pct115
- 726 33. Richardson MW, Hostalek L, Dobson M, Hu J, Shippy R, Siwkowski A, et al.  
727 Design, targeting, and initial screening of sTRSV-derived hairpin ribozymes for  
728 optimum helix 1 length and catalytic efficiency in vitro. *Methods in Molecular*  
729 *Biology (Clifton, N.J.)*. Springer Nature; 2004. pp. 33958. doi:10.1385/1-59259-746-  
730 7:339
- 731 34. Nelson JA, Shepotinovskaya I, Uhlenbeck OC. Hammerheads derived from sTRSV  
732 show enhanced cleavage and ligation rate constants. *Biochemistry*. American  
733 Chemical Society (ACS); 2005. pp. 1457785. doi:10.1021/BI051130T
- 734 35. Deuschle U, Kammerer W, Gentz R, Bujard H. Promoters of Escherichia coli: a  
735 hierarchy of in vivo strength indicates alternate structures. *The EMBO Journal*.  
736 EMBO; 1986. pp. 298794. doi:10.1002/J.1460-2075.1986.TB04596.X
- 737 36. Larson CL, Martinez E, Beare PA, Jeffrey B, Heinzen RA, Bonazzi M. Right on Q:  
738 genetics begin to unravel Coxiella burnetii host cell interactions. *Future*



- 739 Microbiology. Future Medicine; 2016. pp. 91939. doi:10.2217/FMB-2016-0044  
740 37. Howard L, Orenstein NS, King NW. Purification on renografin density gradients of  
741 Chlamydia trachomatis grown in the yolk sac of eggs. Appl Microbiol. 1972;27:  
742 102106. Available:  
743 [http://eutils.ncbi.nlm.nih.gov/entrez/eutils/elink.fcgi?dbfrom=pubmed&id=48556](http://eutils.ncbi.nlm.nih.gov/entrez/eutils/elink.fcgi?dbfrom=pubmed&id=4855645&retmode=ref&cmd=prlinks)  
744 [45&retmode=ref&cmd=prlinks](http://eutils.ncbi.nlm.nih.gov/entrez/eutils/elink.fcgi?dbfrom=pubmed&id=4855645&retmode=ref&cmd=prlinks)  
745 38. Grieshaber NA, Runac J, Turner S, Dean M, Appa C, Omsland A, et al. The sRNA  
746 Regulated Protein DdbA Is Involved in Development and Maintenance of the  
747 Chlamydia trachomatis EB Cell Form. Frontiers in Cellular and Infection  
748 Microbiology. Frontiers Media S.A.; 2021. doi:10.3389/FCIMB.2021.692224  
749 39. Tinevez J-Y, Perry N, Schindelin J, Hoopes GM, Reynolds GD, Laplantine E, et al.  
750 TrackMate: An open and extensible platform for single-particle tracking. Methods.  
751 Academic Press; 2015;115: 8090. doi:10.1016/j.ymeth.2016.09.016  
752 40. Langdon WB. Performance of genetic programming optimised Bowtie2 on genome  
753 comparison and analytic testing (GCAT) benchmarks. BioData Min. Department of  
754 Computer Science University College London, Gower Street, London, WC1E 6BT  
755 UK.: BioMed Central; 2013;8: 1. doi:10.1186/s13040-014-0034-0  
756 41. Anders S, Pyl PT, Huber W. HTSeq--a Python framework to work with high-  
757 throughput sequencing data. Bioinforma. 31: 166169.  
758 doi:10.1093/bioinformatics/btu638  
759 42. Love MI, Huber W, Anders S. Moderated estimation of fold change and dispersion  
760 for RNA-seq data with DESeq2. Genome Biol. BioMed Central; 2012;15: 550.  
761 doi:10.1186/s13059-014-0550-8  
762 43. Haslwanter T. An Introduction to Statistics with Python: With Applications in the Life  
763 Sciences 2013. Available:  
764 [http://books.google.com/books?hl=en&lr=&id=ZBi1DAAAQBAJ&oi=fnd&pg=PR7&d](http://books.google.com/books?hl=en&lr=&id=ZBi1DAAAQBAJ&oi=fnd&pg=PR7&dq=seaborn+python&ots=47D22VZUbM&sig=GPJ6-XGP0EjLwWnQI17BI_fp0SY)  
765 [q=seaborn python&ots=47D22VZUbM&sig=GPJ6-XGP0EjLwWnQI17BI\\_fp0SY](http://books.google.com/books?hl=en&lr=&id=ZBi1DAAAQBAJ&oi=fnd&pg=PR7&dq=seaborn+python&ots=47D22VZUbM&sig=GPJ6-XGP0EjLwWnQI17BI_fp0SY)  
766  
767



768 **Supporting information:**

769

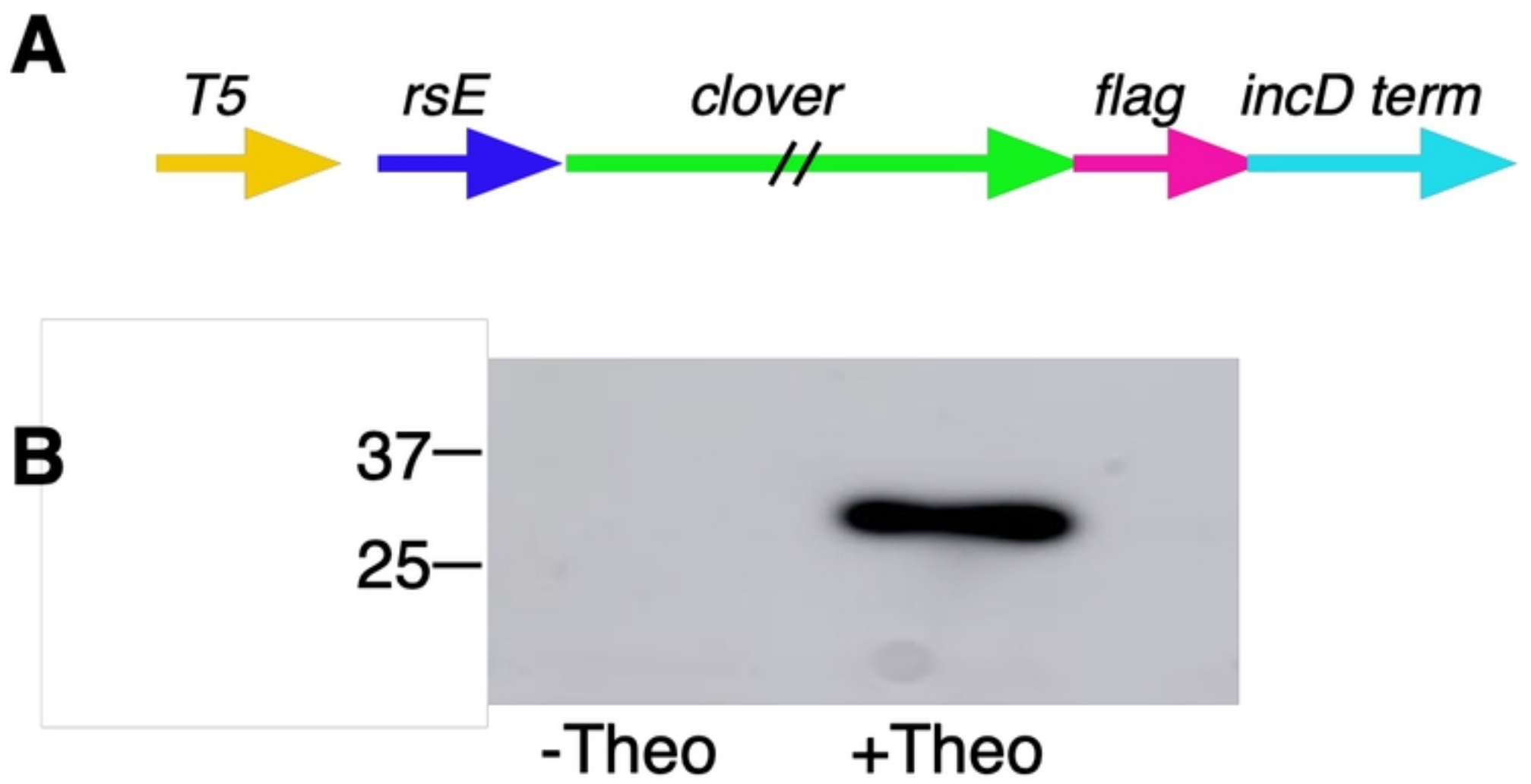
770 **Figure S1. IFU results at 30 hpi.** A) Cos-7 cells were infected with L2-T5-E-clover-flag  
771 and the production of infectious progeny was determined at 30 hpi after theophylline  
772 induction or vehicle only. B) Cos-7 cells were infected with L2-nprom-E-pgp4-flag and the  
773 production of infectious progeny was determined at 30 hpi after theophylline induction or  
774 vehicle only. C) Cos-7 cells were infected with L2-Tet-J-E-clover-flag and the production  
775 of infectious progeny was determined at 30 hpi after induction with 0.5 mM theophylline,  
776 30ng/ml aTc, both aTc and theophylline or vehicle only at 16 hpi. D) Cos-7 cells were  
777 infected with L2-Tet-J-E-hctB-flag and the production of infectious progeny was  
778 determined at 30 hpi after induction with 0.5 mM theophylline, 30ng/ml aTc, both aTc and  
779 theophylline or vehicle only at 16 hpi. Asterisks denote p-values < 0.05. Error bars = SEM.

780

781 **Figure S2. RNA-seq analysis of p2TK2-SW2-Tetprom-riboJ-E-hctB-flag.** Cos-7 cells  
782 infected with L2-Tet-J-E-hctB-flag were induced with 0.5 mM theophylline and 30ng/ml  
783 aTc at 15 hpi and RNA was harvested at 24 hpi. RNA was processed for next-gen RNA-  
784 seq sequencing. Aligned reads are shown with the schematic of the Tet-J-E-hctB.

785

786 **Table ST1.** Primers and templates used for plasmid construction.



bioRxiv preprint doi: <https://doi.org/10.1101/2021.08.31.458335>; this version posted August 31, 2021. The copyright holder for this preprint (which was not certified by peer review) is the author/funder, who has granted bioRxiv a license to display the preprint in perpetuity. It is made available under aCC-BY 4.0 International license.

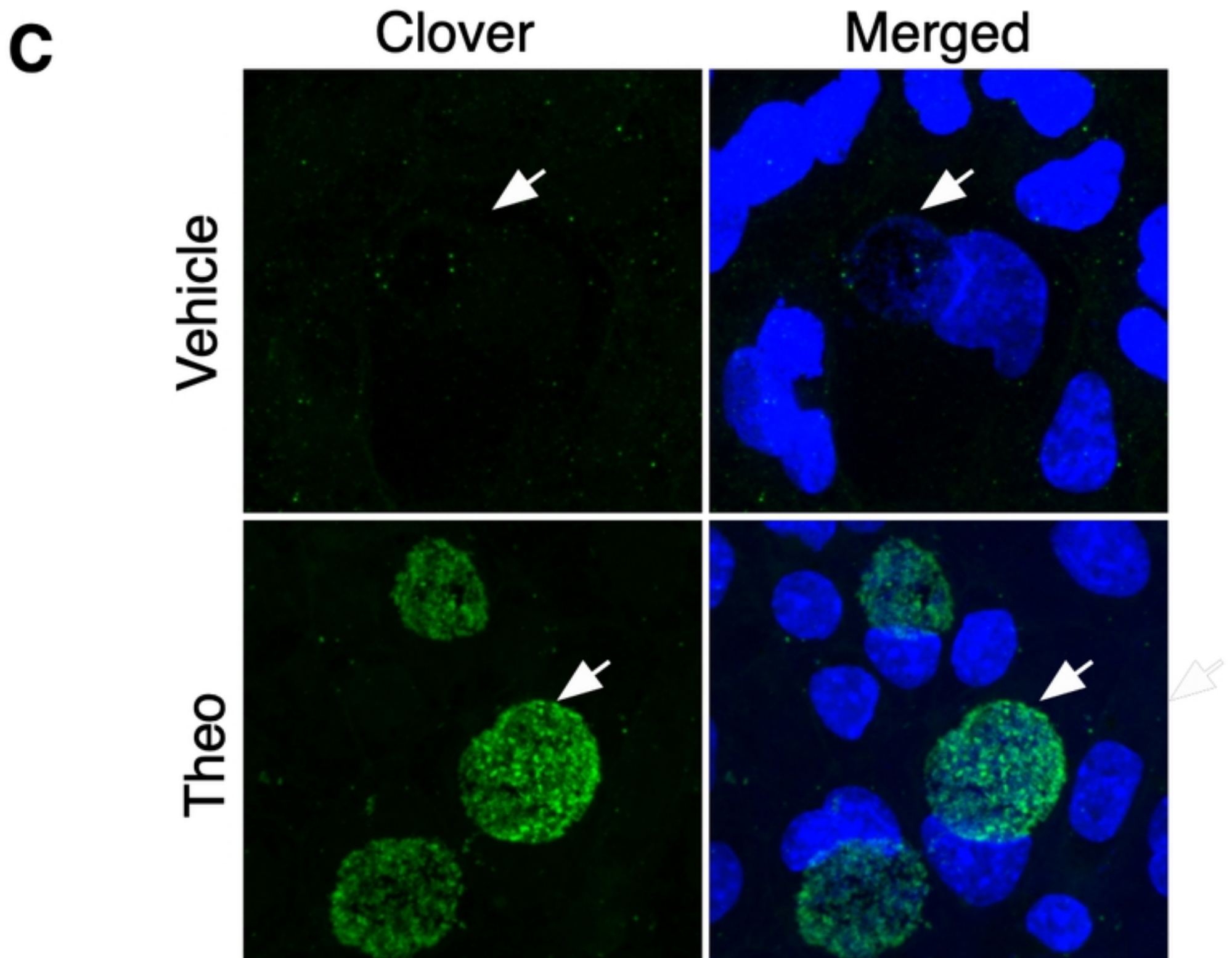


Figure 1

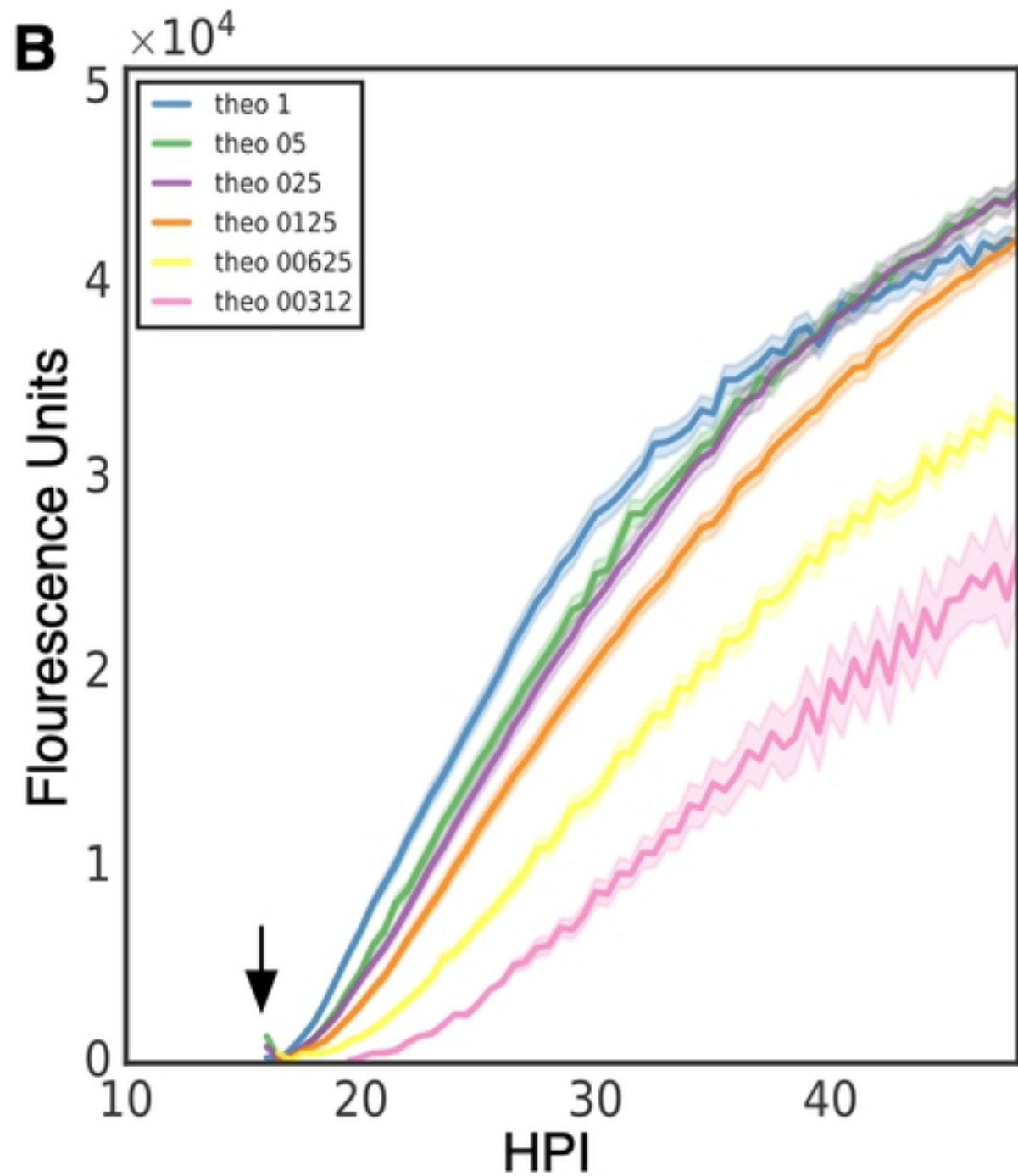
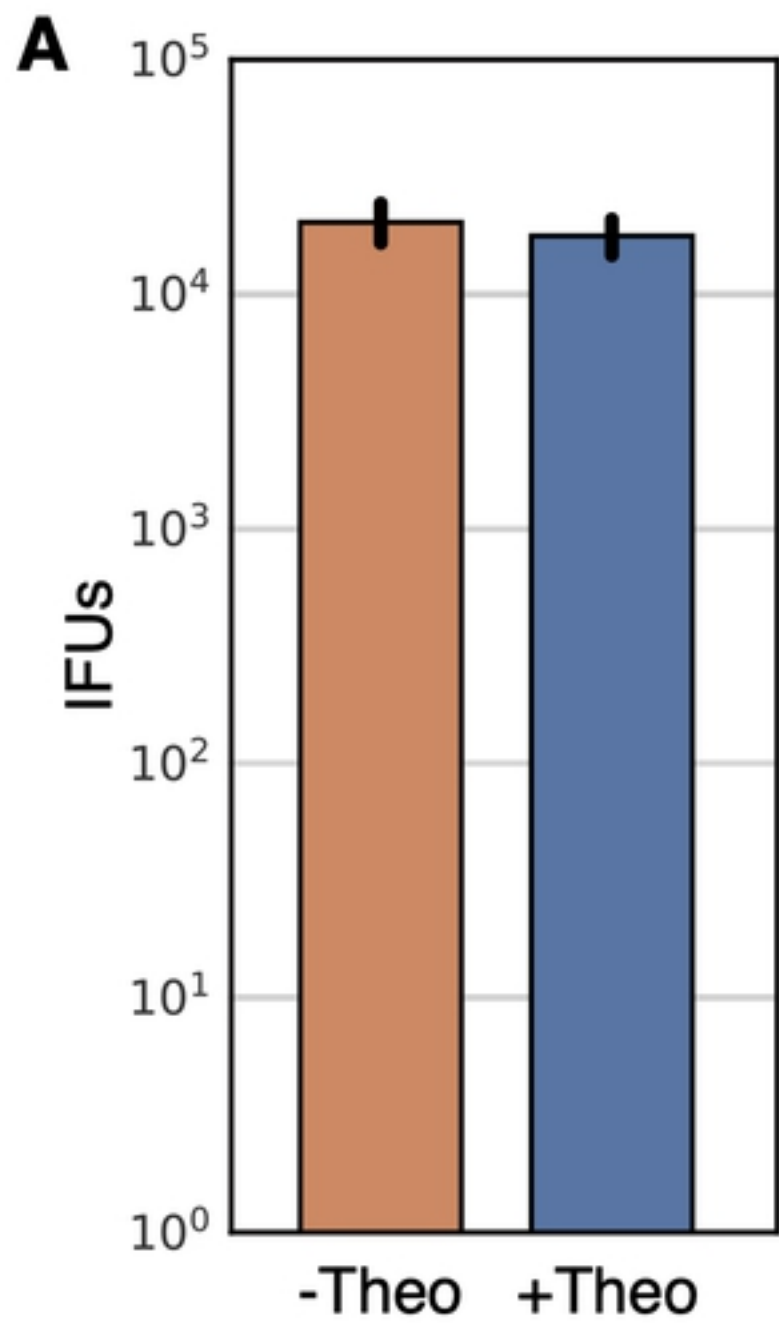


Figure 2



bioRxiv preprint doi: <https://doi.org/10.1101/2021.08.31.458335>; this version posted August 31, 2021. The copyright holder for this preprint (which was not certified by peer review) is the author/funder, who has granted bioRxiv a license to display the preprint in perpetuity. It is made available under aCC-BY 4.0 International license.

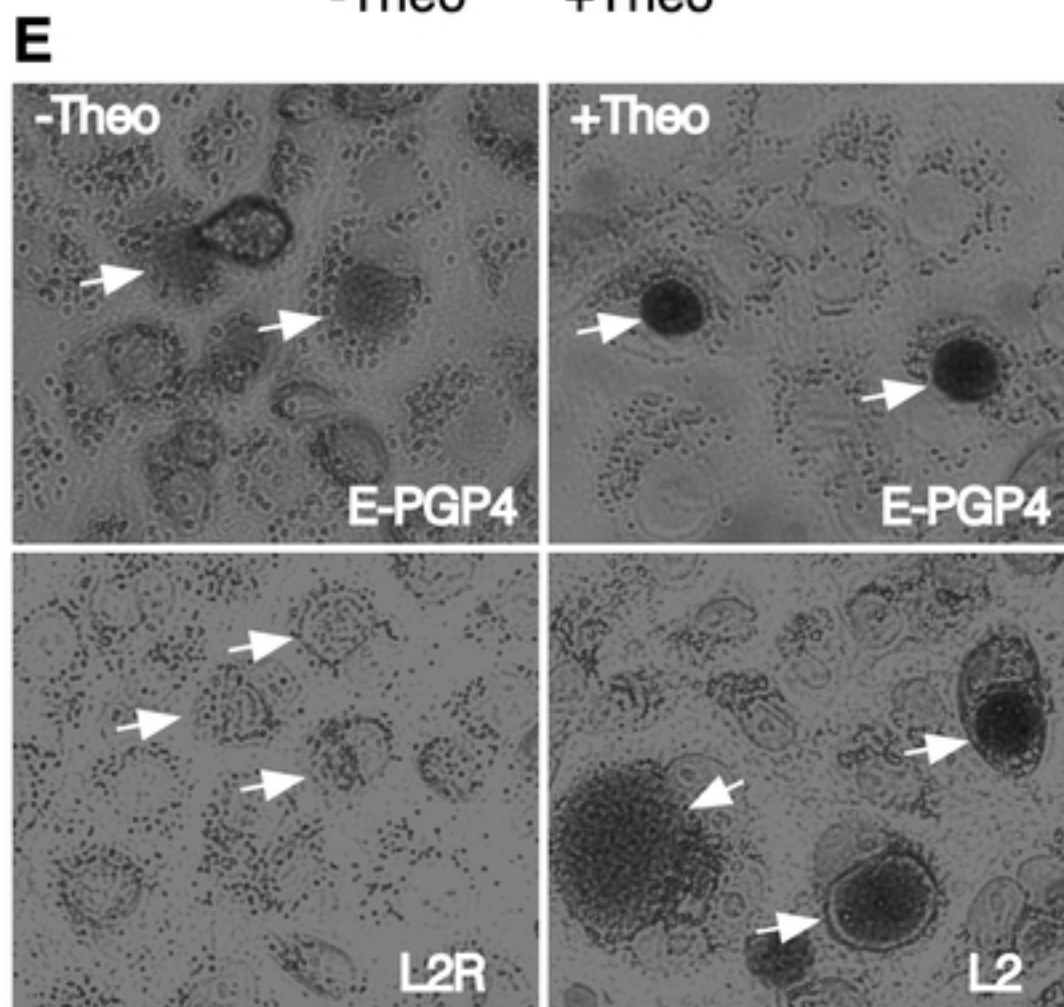
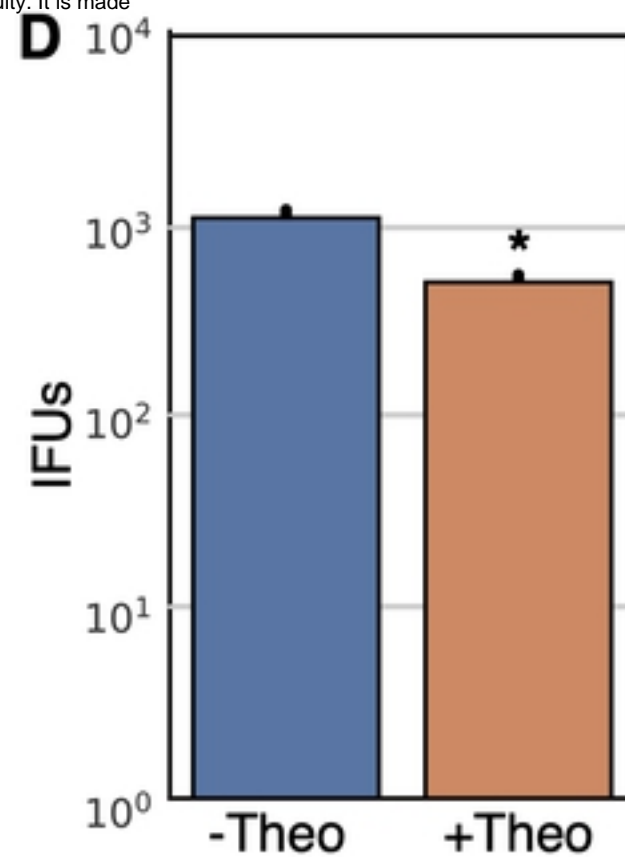
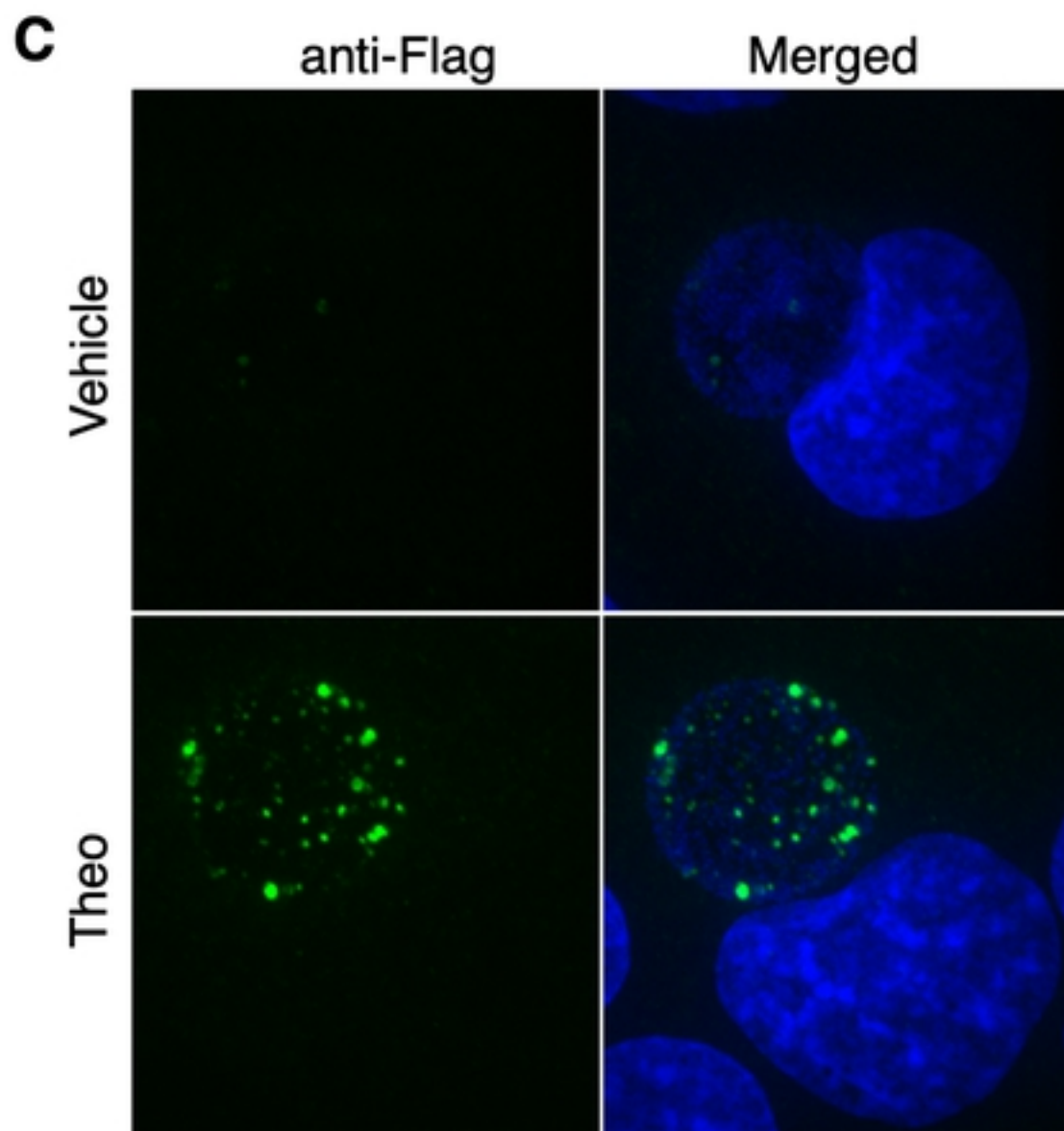
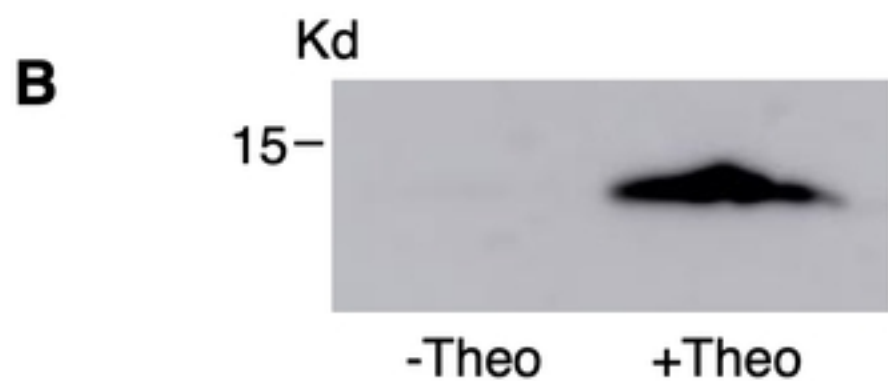


Figure 3



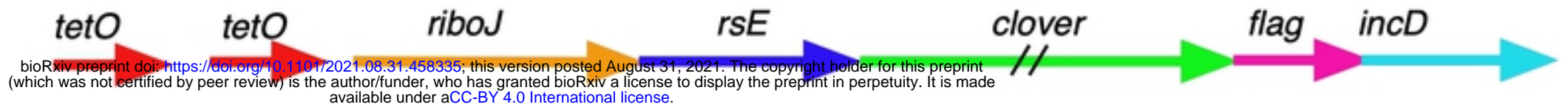
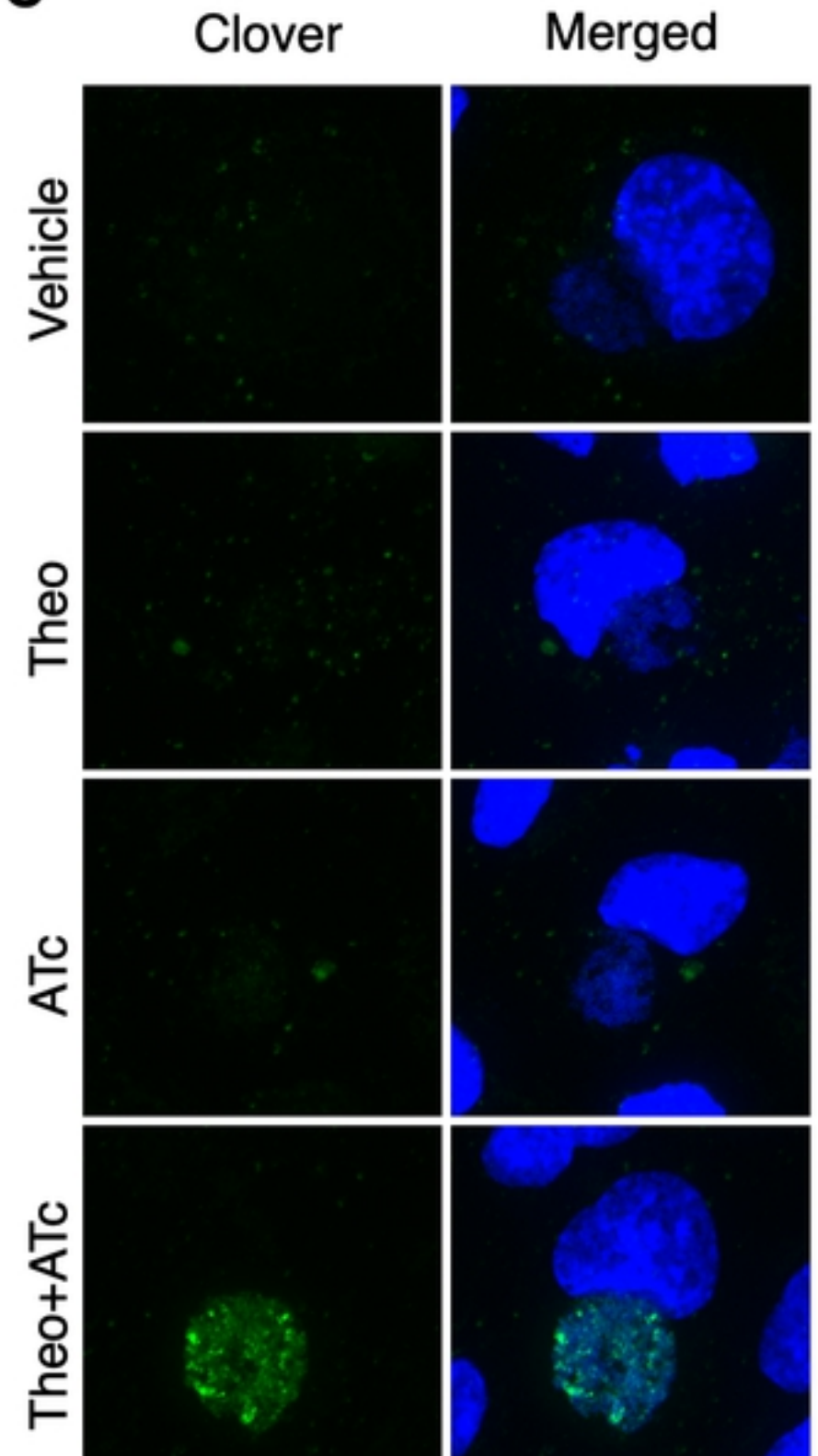
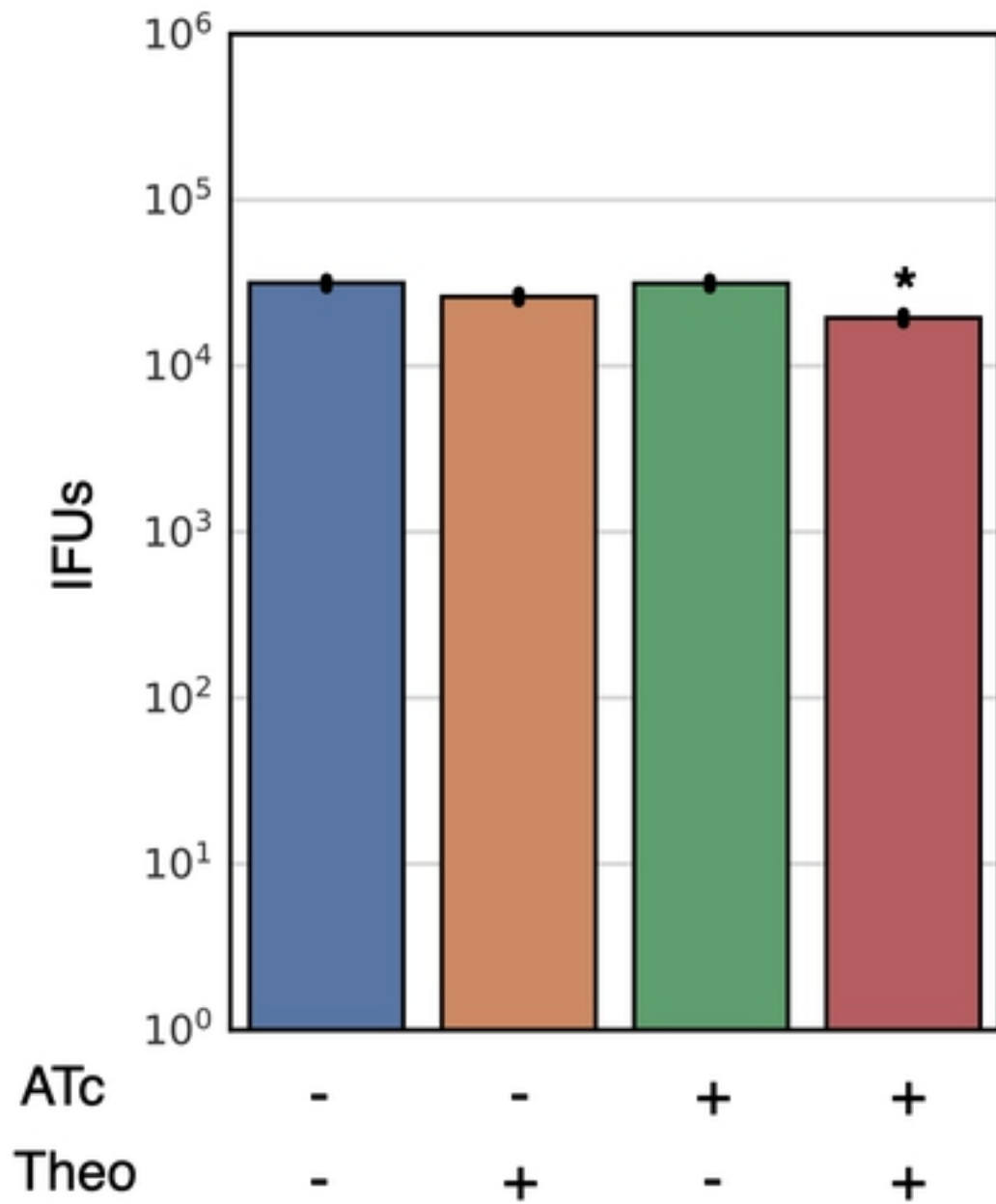
**A****B****C****D**

Figure 4

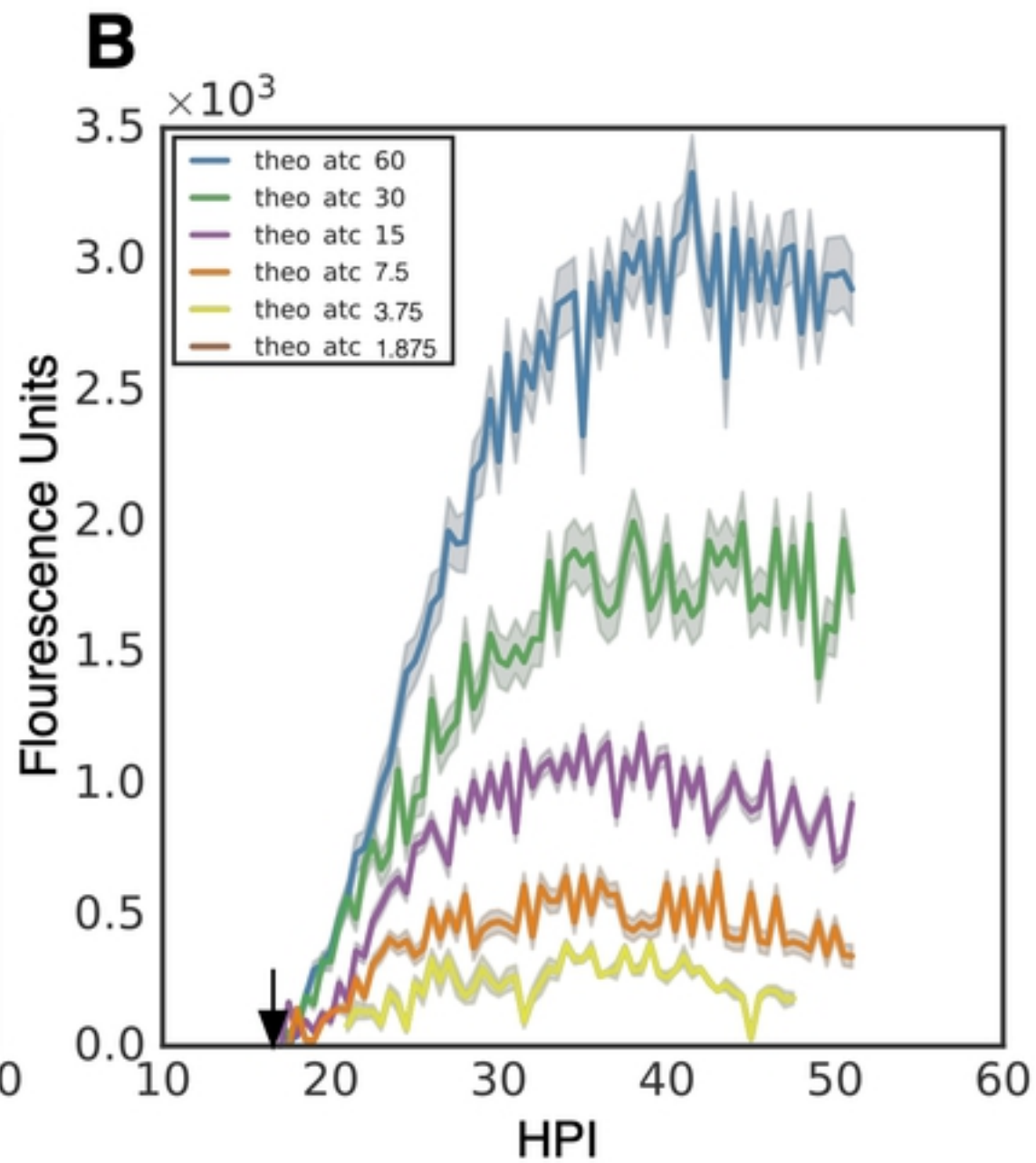
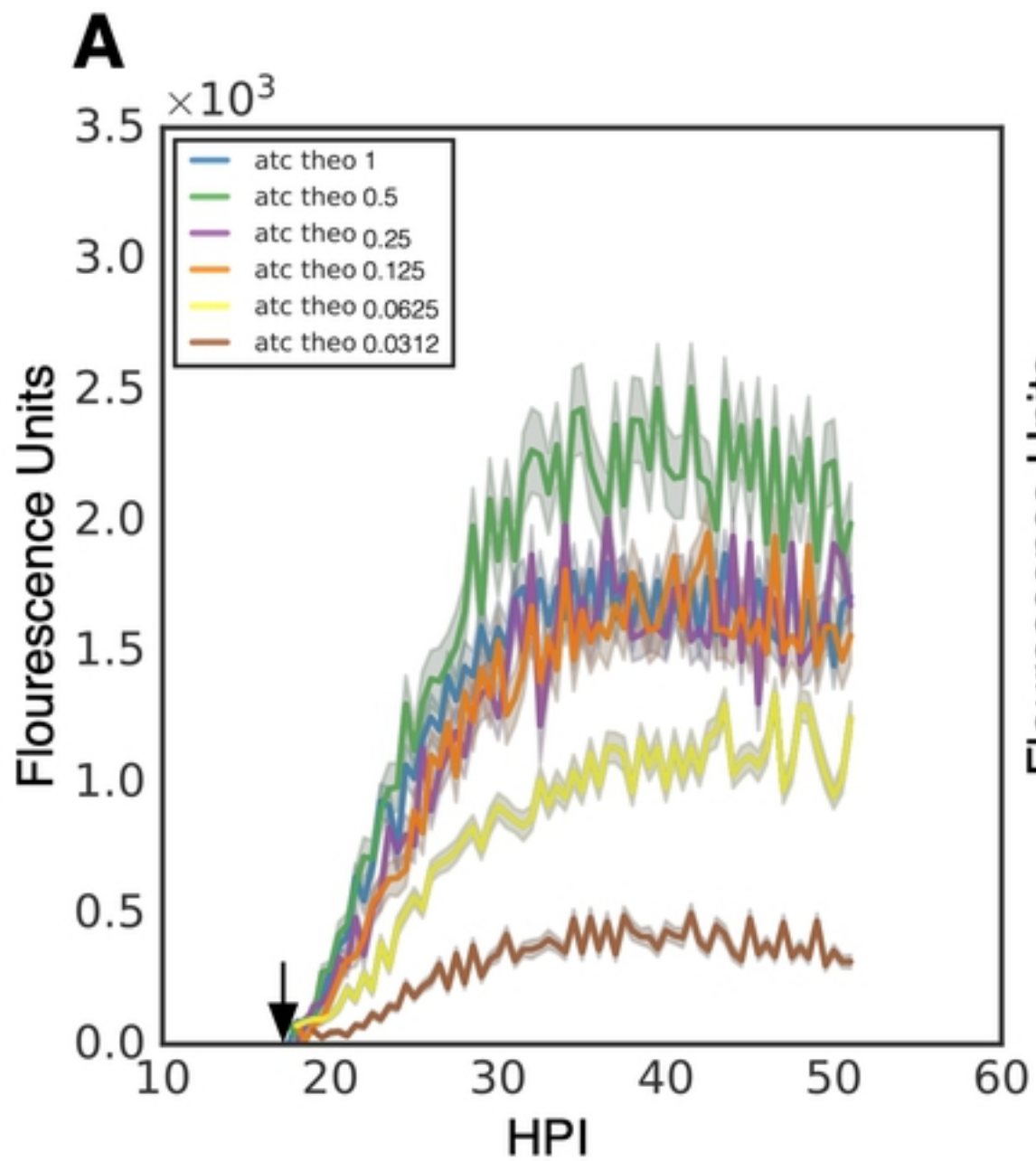


Figure 5



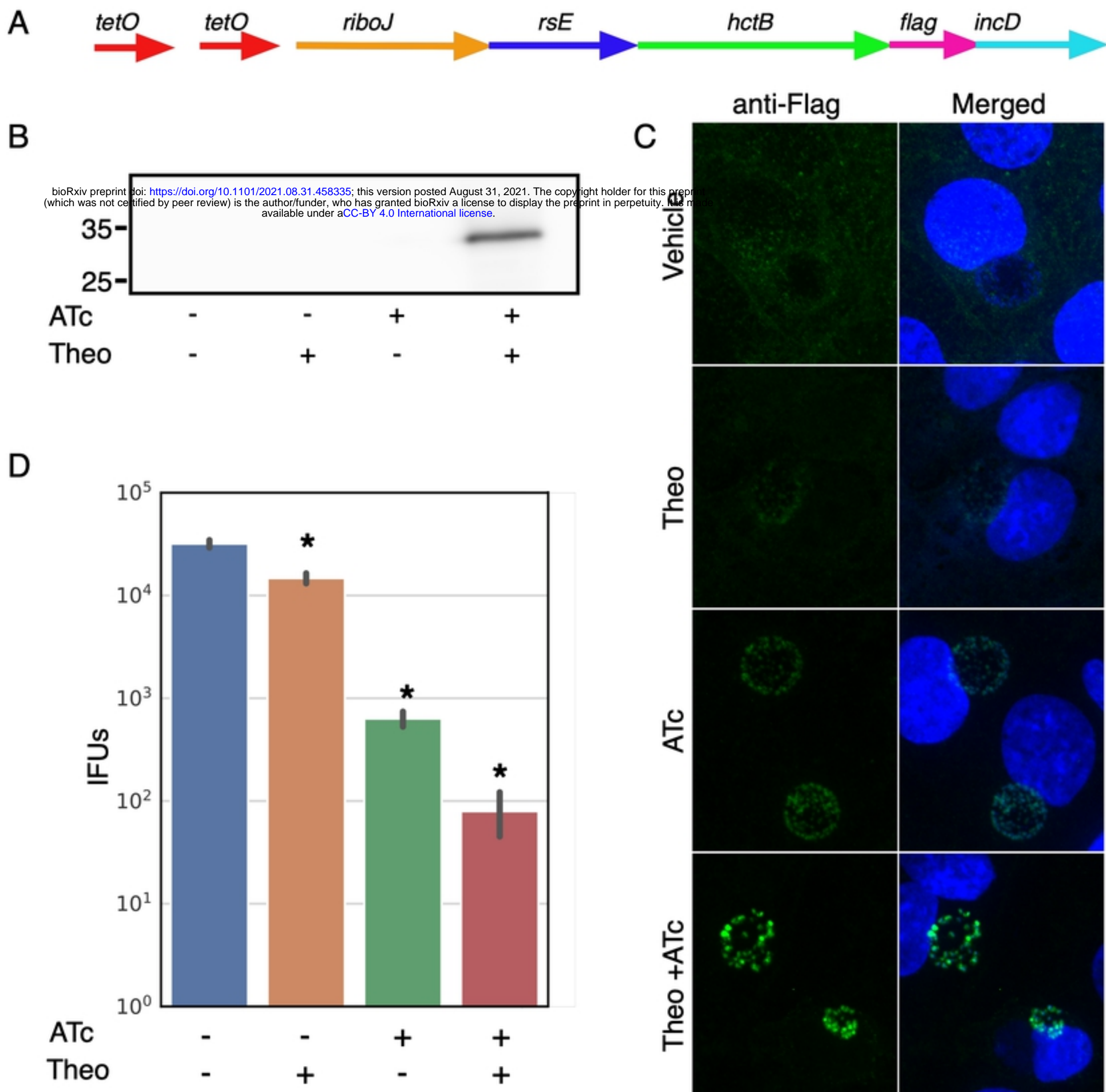
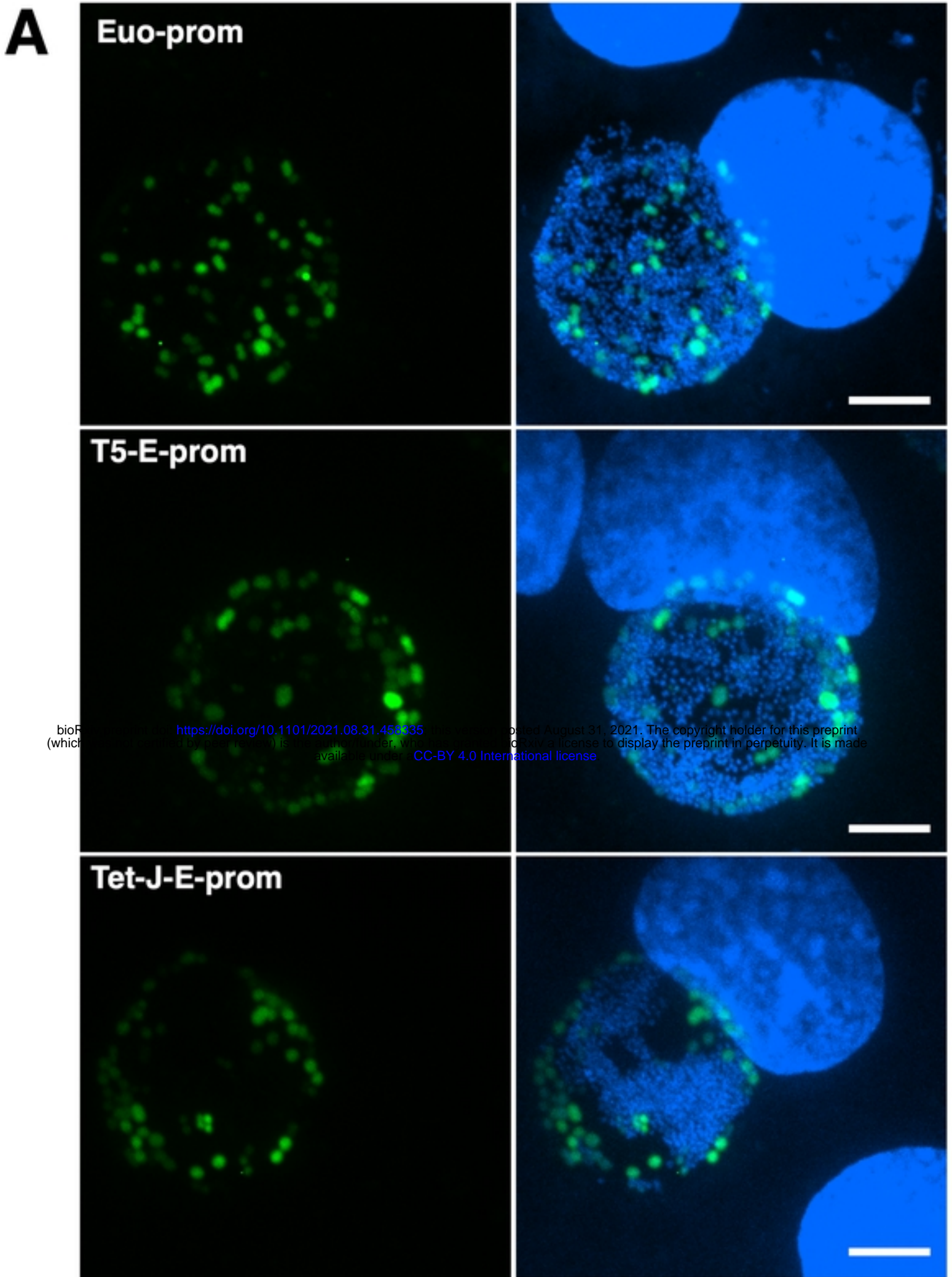


Figure 6



**B**

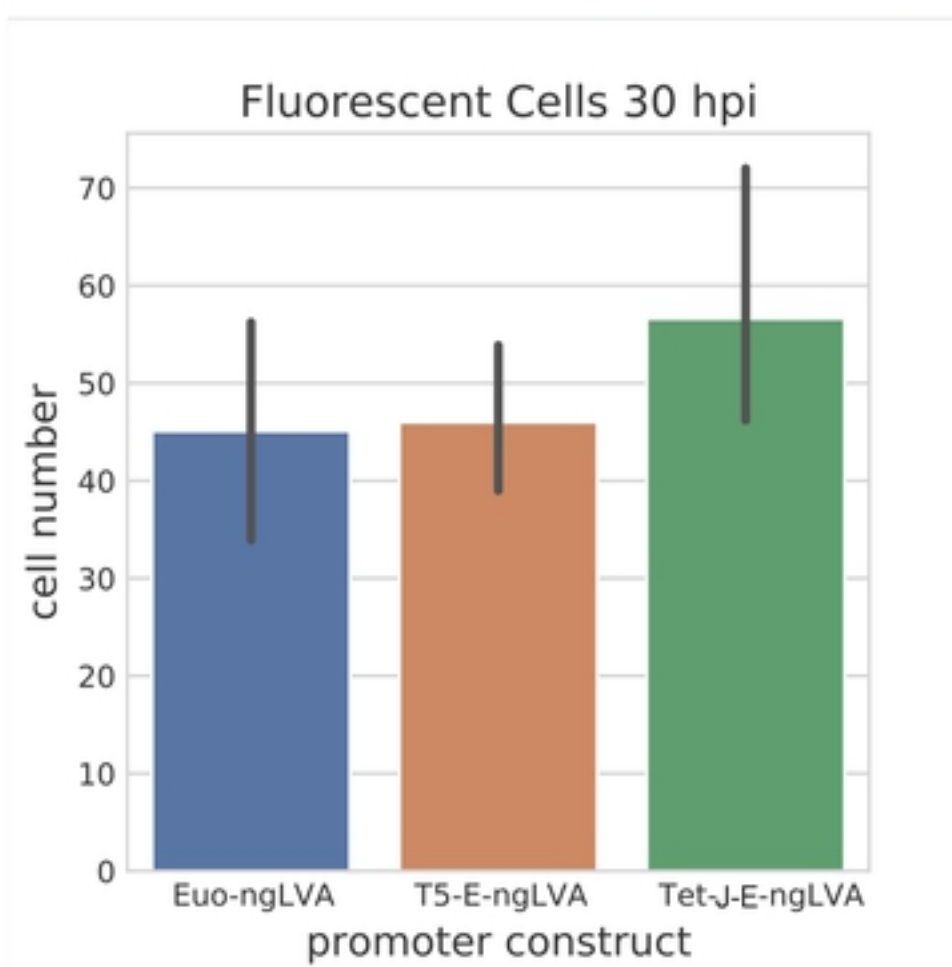


Figure 7